

Radial pulsations of a fluid sphere in a sound wave

By S. TEMKIN

Department of Mechanical and Aerospace Engineering, Rutgers University, 98 Brett Road,
Piscataway, NJ 08854-8058, USA

(Received 6 January 1997 and in revised form 18 August 1998)

This paper presents analytical results for the temperature and pressure fluctuations in a droplet or bubble pulsating in a sound wave, the related damping coefficients, as well as the corresponding sound attenuation coefficients for dilute suspensions. The study is limited to small-amplitude motions but includes the effects of compressibility and heat conduction in the fluid outside the particle. Results are obtained for both average and surface values of the particle's temperature and pressure fluctuations that are applicable to droplets in gases and liquids, and to gas bubbles in liquids. In the latter instance, it is found that the bubble's response exhibits a clear resonant peak at the isothermal natural frequency, that acoustic radiation is the dominant dissipation mechanism near resonance, and that the disturbances produced by the bubble in the liquid significantly reduce the thermal damping at most frequencies. Similar conclusions apply for droplets in liquids, except that the effects of resonance are significantly diminished.

1. Introduction

It is well known that small gas bubbles in liquids can easily be made to oscillate radially by small-amplitude sound waves. Such motions are important in a variety of contexts, for example in the determination of bubble sizes in bubble clouds from acoustic measurements (Medwin 1977), and in cavitation studies (Prosperetti 1986). Although the response of droplets to sound waves is less spirited, they can also execute radial oscillations, particularly in liquids. However, the literature on droplets in sound waves is largely concerned with the attenuation of sound in emulsions resulting from translational motions (see, for example, the extensive bibliography cited by Allegra & Hawley 1972, and shorter, but more recent surveys given by McClements & Povey 1989, and by Fukumoto & Izuyama 1992). In the case of liquid-droplet aerosols, the radial motions can be usually ignored because the droplet's compressibility, being much smaller than that of the gas outside, makes them appear as rigid. But in the case of droplets in liquids, the compressibilities are comparable so that it is likely that radial motions are excited. These may produce additional energy losses, acoustic radiation for example, but this does not seem to have been studied. In the case of gas bubbles, these effects have been studied by many investigators, notably Prosperetti (see, for example, Prosperetti 1977, 1986, 1991) who has calculated the thermal losses on the assumption that the liquid temperature remains constant. One basis for this assumption is the vast differences between the thermal properties of the gas and the liquid.

For droplets in liquids, on the other hand, the properties have comparable values, making it necessary to retain the temperature fluctuation in the liquid. This is

substantiated by an order of magnitude analysis. But, in addition, the same analysis shows that even for gas bubbles in liquids it is not generally possible to neglect those fluctuations.

For these reasons, we have studied the radial response of a small fluid sphere to a sound wave in an otherwise unbounded fluid. The study includes only those aspects of the problem that are essential to the problem at hand and neglects others that may be important in some contexts, for example mass transfer (see, for example, Marble 1970; Cole & Dobbins 1970; Nigmatulin, Khabeev & Zuong Ngok Hai 1988, and Gumerov, Ivanadev & Nigmatulin 1988). The analysis is similar to that of Epstein & Carhart 1953, referred to as E & C hereafter), except that we consider only that part of the incident wave that is uniform around the sphere, that is, the $n = 0$ mode in a spherical-harmonic representation of a plane wave. The remaining modes are needed to study other motions of the sphere, translational, for example. But in the linear approximation these motions are decoupled so that they can be studied separately.

The theory is used to obtain explicit results for the pressure and temperature fluctuations in the particle, and to compute energy dissipation rates due to acoustic radiation and to thermal dissipation. These rates are used to study the attenuation of sound in dilute suspensions, and the acoustic and thermal damping coefficients for a gas bubble in a liquid. In the attenuation case, we compare our thermal attenuation results to those of E & C, and find that disagreement exists. We show that the reason for this is that the explicit formulas for thermal attenuation given by these and by other investigators (e.g. Isakovich 1948; Allegra & Hawley 1972), do not take into account the pressure disturbance in the liquid.

In the second application, damping of gas bubbles in liquids, we find that our thermal damping is significantly different from that found in the literature. We ascribe the differences to the temperature fluctuations in the liquid, and to the disturbance pressure field produced by the pulsating particle.

2. Basic equations

2.1. Background motion

We wish to consider linear, forced pulsations that are produced by a plane, monochromatic sound wave, of circular frequency ω , propagating in a fluid of infinite extent. In the absence of the particle (droplet or bubble), this wave can be treated as an ideal acoustic wave; that is, as a wave that propagates without attenuation or dispersion. We further assume that the wavelength is sufficiently long that the background field can be considered uniform around the sphere. In the absence of the particle, the pressure, temperature and density fluctuations can then be expressed as the real parts of

$$P'_f = P'_{f0} e^{-i\omega t}, \quad \Theta'_f = \Theta'_{f0} e^{-i\omega t}, \quad \Delta'_f = \Delta'_{f0} e^{-i\omega t}, \quad (2.1)$$

respectively, where P'_{f0} , Θ'_{f0} and Δ'_{f0} real. In view of the large number of symbols used in this paper, a list is given in Appendix D. Since the field in the absence of the particle is ideal, these fluctuations are related by the ideal acoustic equations. Thus,

$$P'_f = (\rho_{f0} c_{pf} / \beta_f T_0) \Theta'_f = c_{sf}^2 \Delta'_f, \quad (2.2)$$

where c_{pf} , β_f , and c_{sf} are, respectively, the specific heat at constant pressure, coefficient of thermal expansion, and isentropic sound speed of the fluid. Further, the fluctuations satisfy the usual, small-amplitude requirements $\Delta'_f \ll \rho_{f0}$, $\Theta'_f \ll T_0$, and $P'_f \ll \rho_{f0} c_{sf}^2$ where T_0 and ρ_{f0} are the ambient temperature and density.

2.2. Equations of motion

We now consider the motions that result when a compressible fluid particle is placed in the uniform fluctuating field described by (2.1). These are a disturbance produced by the particle in the fluid outside, as well as a fluctuation in the particle produced by the background motion outside. Both motions are, of course centrally-symmetric if the particle is spherical, which we assume to be the case. We also assume that they satisfy the Navier–Stokes equations. When the amplitudes of all fluctuations are small, the motions are described by the acoustic equations for viscous heat-conducting fluids. These are (see, for example, Temkin 1981)

$$\frac{\partial \rho'}{\partial t} + \rho_0 \nabla \cdot \mathbf{u} = 0, \quad (2.3)$$

$$\rho_0 \frac{\partial \mathbf{u}}{\partial t} + \nabla p' = \frac{4}{3} \mu \nabla (\nabla \cdot \mathbf{u}) - \mu \nabla \times (\nabla \times \mathbf{u}), \quad (2.4)$$

$$\rho_0 c_p \frac{\partial T'}{\partial t} - \beta T_0 \frac{\partial \rho}{\partial t} = k \nabla^2 T'. \quad (2.5)$$

The equation of state for both fluids completes the set. Thus

$$p' = c_T^2 p' + \frac{\rho_0 c_p}{\beta T_0} \frac{\gamma - 1}{\gamma} T', \quad (2.6)$$

where γ is the specific heat ratio, β is the coefficient of thermal expansion, c_T is the isothermal sound speed, c_p is the specific heat at constant pressure, k is the thermal conductivity, and μ is the viscosity. Since the main equations and the properties appearing in them apply to either fluid, we shall use the additional suffixes p and f to denote the fluid in the particle and that outside it, respectively. For example, the conductivity of the fluids in the particle and outside will be denoted by k_p and k_f , respectively, in which case the symbol k can be used to denote the wavenumber in the undisturbed field.

The above system of equations applies to both fluids and is complemented by the usual boundary conditions on the velocity, pressure, temperature and heat flux. When the particle is a sphere, the motions are along the radial direction so that the two velocity vectors have only one component each, which is along the radial direction. That is $\mathbf{u}_p = \{u_p, 0, 0\}$, $\mathbf{u}_f = \{u_f, 0, 0\}$.

Although this system and the boundary conditions that it satisfies are linear, further simplification is necessary owing to the large number of variables. We have already restricted the study to waves whose length is larger than the particle size. Below we show that for frequencies such that this restriction applies, the effects of viscosity can be neglected. However, we find it necessary to retain the thermal effects in both fluids, as well as the pressure disturbance produced in the exterior fluid by the pulsating particle. The latter is examined in §4, where it is shown that its effects are significant at all frequencies but the smallest, particularly in the case of gas bubbles in liquids.

Here, we consider the temperature fluctuation, noting that, for gas bubbles in liquids, past investigators have neglected the temperature fluctuations in the external fluid, on the assumption that it is always very small. Indeed, we find that to be the case in a limited range of frequencies. But for droplets in gases or in liquids, or for gas bubbles at low or high frequencies, it is not possible to disregard those fluctuations. To show this, we consider the changes of temperature in the particle and in the fluid, relative to those at the surface of the particle, T'_s . As sketched in figure 1, the particle produces a temperature disturbance, θ'_f , which at far distances from it has a very

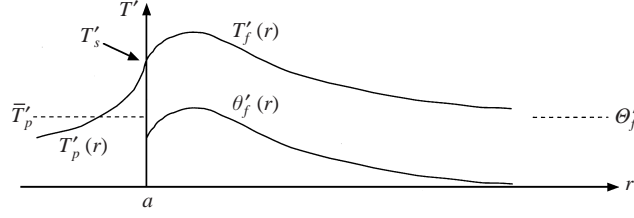


FIGURE 1. Schematic representation of the temperature fields inside and outside the spherical particle θ'_f is the temperature disturbance in the fluid, and \bar{T}'_p is an average temperature in the particle, defined in §3.

small amplitude at all finite frequencies. Hence, the temperature fluctuation at such distances is simply Θ'_f , the value prescribed by its value in the sound wave. This varies from case to case, and is usually very small for liquids. But so long as the specific heat ratio of the fluid outside is larger than unity (as prescribed by thermodynamics), the amplitude of temperature fluctuation in the liquid far from the particle is never zero. On the other hand, at the surface of the particle, the disturbance is finite. Hence, except for the limiting condition $\omega \rightarrow 0$, where the temperature is uniform throughout, T'_s and Θ'_f are different. Consider now the fluid in the particle. The temperature, T'_p , at some point in it depends on the value of the thermal penetration depth, δ_{κ_p} , relative to the radius of the particle, a , and it is necessary to consider three separate cases: $\delta_{\kappa_p} \gg a$, $\delta_{\kappa_p} = O(a)$, and $\delta_{\kappa_p} \ll a$. Since $\delta_{\kappa_p} = (2\kappa_p/\omega)^{1/2}$ where κ_p is the thermal diffusivity of the fluid in the particle, these correspond, respectively, to low, moderate, and high frequencies.

At low, but finite, frequencies, the thermal wave is able to equalize the temperature field within the particle in a very short fraction of the period of the oscillation. Hence, the instantaneous temperature difference between any point in the particle and the surface value is exceedingly small, or $T'_p \approx T'_s$. On the other hand, as shown above, the external temperature difference, $T'_s - \Theta'_f$, is finite (and, in fact, it is this difference that prescribes the instantaneous value of T'_p). Hence at low frequencies, we cannot neglect the external temperature field.

Consider now the case $\delta_{\kappa_p} \ll a$, corresponding to high frequencies. It is clear that the temperature fluctuation will be negligible at most points in the particle, and that the temperature fluctuation beyond a small distance outside it will be equal to Θ'_f . Thus, at high frequencies, it is also not possible to ignore the temperature field outside.

Finally, we consider the intermediate case, $\delta_{\kappa_p} = O(a)$. Following Prosperetti (1986) we estimate the order of magnitude of the temperature fluctuations from the condition that the heat fluxes at the boundary be equal. In this frequency range, the length scales in both fluids are the corresponding thermal penetration depths, δ_{κ_p} for the particle and $\delta_{\kappa_f} = (2\kappa_f/\omega)^{1/2}$ for the fluid outside. We thus find that the heat fluxes are of the order of $k_f(\omega/2\kappa_f)^{1/2}(T'_s - \Theta'_f)$, for the fluid, and $k_p(\omega/2\kappa_p)^{1/2}(T'_s - T'_p)$ for the particle. Thus, the condition on the heat fluxes gives the estimate

$$\frac{|T'_s - T'_p|}{|T'_s - \Theta'_f|} \sim \left\{ \frac{k_f \rho_f c_{pf}}{k_p \rho_p c_{pp}} \right\}^{1/2}. \quad (2.7)$$

This applies to the three cases under consideration, namely gas bubbles in liquids, droplets in liquids, and droplets in gases. Because the physical property ratios for each case vary significantly from one to the next (see table 1), the temperature-fluctuation

	Air*	Toluene†	Water*
c_p (J g ⁻¹ K ⁻¹)	1.012	1.652	4.186
c_s (cm s ⁻¹)	3.40×10^4	1.37×10^5	1.48×10^5
β (K ⁻¹)	3.47×10^{-3}	1.04×10^{-3}	1.5×10^{-4}
$\gamma‡$	1.400	1.3564	1.0034
κ (cm ² s ⁻¹)	2.02×10^{-1}	1.11×10^{-3}	1.4×10^{-3}
ρ (g cm ⁻³)	1.23×10^{-3}	0.870	0.9991

* From Batchelor (1967).

† From Allegra & Hawley (1972).

‡ Calculated from the thermodynamic relation $\gamma = 1 + T_0\beta^2 c_s^2 / c_p$.

TABLE 1. Physical properties of some fluids at 1 atm and 15°C.

estimate will also differ from case to case. Thus, for gas bubbles in liquids, the quantity on the right-hand side of (2.7) is of the order of 10^2 , indicating that at such frequencies, the temperature differences within the particle are much larger than those in the fluid. But for a liquid droplet immersed in another liquid, the right-hand side of (2.7) is of order 1, which indicates that the temperature changes inside are of the same order as those outside. And in the case of liquid droplets in gases, the magnitude of the temperature changes inside a droplet is about one-hundredth of the change outside. We therefore conclude that, generally speaking, it is not possible to disregard the temperature fluctuations in the fluid outside the particle.

2.3. Reduction

We now proceed to reduce the eight coupled differential equations to a more manageable system. Thus, because the motions are centrally symmetric, the velocity field is irrotational, and can therefore be obtained from a velocity potential, ϕ , by means of

$$\mathbf{u} = \nabla\phi. \quad (2.8)$$

Further, since the motion is monochromatic, the time dependence occurs only through the factor $\exp(-i\omega t)$. Using these relations in the above system, we obtain, after some manipulations,

$$[\nabla^2 + (ka)^2][\nabla^2 + (Ka)^2]\phi = 0, \quad (2.9)$$

where the wavenumbers k and K are generally complex and are given, approximately, by (Temkin 1981)

$$k = (\omega/c_s)\{1 + i[2\omega\nu/3c_s^2 + (\gamma_f - 1)\omega\kappa/2c_s^2]\} \quad \text{and} \quad K = (1 + i)(\omega/2\kappa)^{1/2}, \quad (2.10a,b)$$

and are such that $|k^2| \ll |K^2|$. This follows from the above equations and from the fact that both $\omega\nu/c_s^2$ and $\omega\kappa/c_s^2$ are very small. These ratios measure the speeds of propagation of thermal and viscous waves, respectively, relative to the isentropic sound speeds, and are essentially equal to the viscous and thermal sound attenuation coefficients in a fluid. At 10 MHz, for example, these quantities are of the order of 10^{-2} in air and smaller still in water, meaning, as is well known, that the attenuation of sound in fluids devoid of boundaries can be usually neglected. The smallness of $|k^2/K^2|$ will also be used later to simplify the analysis. Here, we note that because k

and K are never equal, a solution for ϕ can be obtained by adding the solutions of

$$\nabla^2 \phi_1 + (ka)^2 \phi_1 = 0 \quad \text{and} \quad \nabla^2 \phi_2 + (Ka)^2 \phi_2 = 0. \quad (2.11a,b)$$

These equations describe two different types of waves. The first represents longitudinal waves travelling in a viscous heat-conducting fluid; the second represents highly attenuated thermal waves. Again, owing to the smallness of $\omega\kappa/c_s^2$ and $\omega\nu/c_s^2$, the effects of dissipation on the first wave are very small and can be neglected in a first approximation. Thus, the wavenumber for ϕ_1 becomes real, that is, $k \approx \omega/c_s$. This fact, together with the absence of shear, means that viscous effects are negligible, so that the pressure fields are given by the inviscid acoustic relationship

$$p' = i\rho_0 \omega(\phi_1 + \phi_2). \quad (2.12)$$

The velocities and temperature fields are given by

$$u = \frac{\partial \phi_1}{\partial r} + \frac{\partial \phi_2}{\partial r} \quad \text{and} \quad -\beta\kappa T' = (\gamma - 1)(k/K)^2 \phi_1 - \phi_2. \quad (2.13a,b)$$

3. Solution

We now apply the above system of equations to study the response of a small particle to an imposed field that is fluctuating harmonically in time. That is, far from the sphere the fluid pressure, temperature and density change harmonically in time according to $p_{f\infty} = p_0 + P'_f$, $T_{f\infty} = T_0 + \Theta'_f$, and $\Delta_{f\infty} = \rho_{f0} + \Delta'_f$ where the fluctuations are given by (2.1).

Near the particle, the uniformity of pressure and temperature is disturbed by the particle. The disturbance field satisfies the equations derived in §2. The complete field outside the particle is then given by the superposition of the uniform fields far from the particle plus the disturbance field, together with boundary conditions at the particle surface and far from it. To avoid confusion with the symbols for the complete field, we will denote the disturbance pressure and temperature by π'_f and θ'_f , respectively. Thus, the disturbance field is prescribed by (2.11a, b). The solutions to these, which are zero at infinity, are

$$\phi_1 = Ah_0^{(1)}(kr) e^{-i\omega t} \quad \text{and} \quad \phi_2 = Bh_0^{(1)}(Kr) e^{-i\omega t}, \quad (3.1a,b)$$

where

$$k = \omega/c_{sf}, \quad K = (1 + i)(\omega/2\kappa_f)^{1/2}, \quad (3.2a,b)$$

and where $h_0^{(1)}$ is the spherical Bessel function of order zero and of the first kind. Since $h_0^{(2)}$ is not needed, we drop, for simplicity, the superscript on $h_0^{(1)}$. Thus, the radial velocity is

$$u_f = [Akh'_0(kr) + BKh'_0(Kr)] e^{-i\omega t}, \quad (3.3)$$

where the prime on $h'_0(kr)$ represents a derivative with respect to the argument. Similarly, the pressure and temperature disturbances are

$$\pi'_f = i\rho_{f0}\omega[Ah_0(kr) + Bh_0(Kr)] e^{-i\omega t}, \quad (3.4)$$

$$-\beta_f\kappa_f\theta'_f = [(\gamma_f - 1)(k/K)^2 Ah_0(kr) - Bh_0(Kr)] e^{-i\omega t}. \quad (3.5)$$

Thus, the pressure and temperature outside the particle are given by

$$p'_f = P'_{f0} e^{-i\omega t} + i\rho_{f0} \omega [Ah_0(kr) + Bh_0(Kr)] e^{-i\omega t}, \quad (3.6)$$

$$T'_f = \Theta'_{f0} e^{-i\omega t} - \frac{1}{\beta_f \kappa_f} [(\gamma_f - 1)(k/K)^2 Ah_0(kr) - Bh_0(Kr)] e^{-i\omega t}. \quad (3.7)$$

Let us now consider the field inside the particle. The solutions inside are similar to those outside, except that the radial factors have to satisfy the condition of finiteness at the origin. Hence, the radial dependence inside the particle will be prescribed by j_0 , the Bessel function of the first kind, and of zero order. Thus, the radial velocity in the particle is given by

$$u_p = [Ck_i j'_0(k_i r) + DK_i j'_0(K_i r)] e^{-i\omega t}, \quad (3.8)$$

where

$$k_i = \omega/c_{sp}, \quad K_i = (1+i)(\omega/2\kappa_p)^{1/2}. \quad (3.9a,b)$$

The corresponding pressure and temperature fluctuations are

$$p'_p = i\rho_{p0} \omega [Cj_0(k_i r) + Dj_0(K_i r)] e^{-i\omega t}, \quad (3.10)$$

$$-\beta_p \kappa_p T'_p = [(\gamma_p - 1)(k_i/K_i)^2 Cj_0(k_i r) - Dj_0(K_i r)] e^{-i\omega t}. \quad (3.11)$$

To obtain A , B , C and D , we make use of the linearized boundary conditions. Thus, if T'_s and p'_s are the fluctuations of temperature and pressure at the surface, and u_s is the radial velocity of the surface, those conditions are

$$T'_p = T'_s = \Theta'_f + \theta'_f, \quad p'_p = p'_s = P'_f + \pi'_f, \quad u_p = u_s = u_f. \quad (3.12)$$

In addition, we have the condition on the heat flux

$$k_f \left(\frac{\partial \theta'_f}{\partial r} \right)_{r=a} = k_p \left(\frac{\partial T'_p}{\partial r} \right)_{r=a}. \quad (3.13)$$

The four equations implied by the temperature and pressure boundary conditions may be solved for A , B , C and D . Thus, introducing the notation

$$\left. \begin{aligned} b_i &= k_i a, & b &= ka \\ q_i &= K_i a, & q &= Ka \end{aligned} \right\} \quad (3.14)$$

we have

$$A = [(p'_s - P'_f)/i\rho_{f0} \omega - \beta_f \kappa_f (T'_s - \Theta'_f)]/h_0(b), \quad B = B_f \kappa_f (T'_s - \Theta'_f)/h_0(q), \quad (3.15a,b)$$

$$C = [p'_s/i\rho_{p0} \omega - T'_s \beta_p \kappa_p]/j_0(b_i), \quad D = \beta_p \kappa_p T'_s/j_0(q_i). \quad (3.16a,b)$$

When these are substituted into (3.3)–(3.11), the fields in the particle and outside it will be specified in terms of the surface temperature and pressure fluctuations, which are not yet determined. To obtain them, we can use the condition on the heat flux and on the radial velocities. Consider the latter first. On the fluid side, the surface velocity is prescribed by (3.3). On the particle side, it is prescribed by (3.8), but it is more convenient to obtain it from the continuity equation for the particle. Thus, integrating that equation over the equilibrium volume of the particle, v_p , and using

the divergence theorem, we obtain

$$\bar{\rho}'_p = \frac{3\rho_{p0}}{i\omega a} u_s, \quad (3.17)$$

where

$$\bar{\rho}'_p = \frac{1}{v_p} \int_{\rho_p} \rho'_p(r, t) \, dv. \quad (3.18)$$

For the heat flux on the particle side, we operate in the same manner on the particle's energy equation to obtain

$$k_p \left(\frac{\partial T'_p}{\partial r} \right)_{r=a} = \frac{-i\omega a}{3} (\rho_{p0} c_{pp} \bar{T}'_p - \beta_p T_0 \bar{p}'_p), \quad (3.19)$$

with \bar{T}'_p and \bar{p}'_p defined by equations similar to (3.18) for $\bar{\rho}'_p$. Any of these three quantities can be eliminated in favour of the other two by means of the particle's equation of state, which gives, after integration,

$$\bar{p}'_p = \gamma_p \bar{p}'_p / c_{sp}^2 - \rho_{p0} \beta_p \bar{T}'_p. \quad (3.20)$$

In view of (3.17), the left-hand side of this equation is proportional to the particle's surface velocity. Thus, (3.20) shows that for a given value of that velocity, the particle temperature and pressure are coupled.

The quantities \bar{T}'_p and \bar{p}'_p and $\bar{\rho}'_p$ thus introduced are, at this stage, defined only as mathematical entities. Later, it will be shown that they can serve as useful representations for the temperature, pressure and density fluctuation in the particle over a wide frequency range.

Let us now return to the velocity and heat-flux conditions. Using the above quantities, as well as the velocity in the fluid, we obtain

$$Abh'_0(b) + Bqh'_0(q) = \frac{i\omega a^2}{3\rho_{p0}} [\gamma_p \bar{p}'_p / c_{sp}^2 - \rho_{p0} \beta_p \bar{T}'_p]. \quad (3.21)$$

Substituting here the results for A and B , yields after some algebra

$$\begin{aligned} \rho_{f0} \omega \beta_f \kappa_f (q-b) \Theta'_f + (1-ib) P'_f = \rho_{f0} \omega \beta_f \kappa_f \left[(q-b) T'_s - \frac{1}{3} q^2 \frac{\beta_p}{\beta_f} \bar{T}'_p \right] \\ + [(1-ib) p'_s - \frac{1}{3} \gamma_p b^2 N_s \bar{p}'_p], \end{aligned} \quad (3.22)$$

where

$$N_s = \rho_{f0} c_{sf}^2 / \rho_{p0} c_{sp}^2 \quad (3.23)$$

is the ratio of particle to fluid isentropic compressibilities, and where we have used the identities

$$\frac{bh'_0(b)}{h_0(b)} = -(1-ib) \quad \text{and} \quad \frac{qh'_0(q)}{h_0(q)} = -(1-iq). \quad (3.24)$$

For the heat flux, we first note that the fluid's heat flux can be written as

$$\begin{aligned} k_f \left(\frac{\partial T'_f}{\partial r} \right)_{r=a} = -\frac{\rho_{f0} c_{pf}}{\beta_f a} \{ \beta_f \kappa_f (T'_s - \Theta'_f) (1-iq) \\ - (\gamma_f - 1) (b/q)^2 (1-ib) (p'_s - P'_f) / i\rho_{f0} \omega \}, \end{aligned} \quad (3.25)$$

where we have neglected a term of order $(b/q)^2$ compared to unity. Equating this to (3.19) gives

$$\begin{aligned} & [\beta_f \kappa_f (T'_s - \Theta'_f)(1 - iq) - (\gamma_f - 1)(b/q)^2(1 - ib)(p'_s - P'_f)/i\rho_{f0}\omega] \\ & = \frac{i\omega a^2 \beta_f}{3\rho_{f0}c_{pf}} [\rho_{p0}c_{pp} \bar{T}'_p - \beta_p T_0 \bar{p}'_p]. \end{aligned} \quad (3.26)$$

Relationships between \bar{T}'_p and \bar{p}'_p as well as among the corresponding surface values may be obtained from the known spatial variations of the temperature and pressure in the particle. Thus, from (3.10) and (3.11), we find upon integration

$$\bar{p}'_p/i\rho_{p0}\omega = -3C j'_0(b_i)/b_i - 3D j'_0(q_i)/q_i, \quad (3.27)$$

$$-\beta_p \kappa_p T'_p = -3(\gamma_p - 1)(b_i/q_i)^2 C j'_0(b_i)/b_i - 3D j'_0(q_i)/q_i. \quad (3.28)$$

Using (3.16 a, b) for C and D , and taking advantage of the smallness of $(b_i/q_i)^2$, we obtain

$$T'_s = \frac{1}{3} q_i^2 G(q_i) \bar{T}'_p, \quad (3.29)$$

where

$$G(q_i) = \frac{j_0(q_i)}{q_i j'_0(q_i)} = \frac{\tanh[(1-i)z_p]}{(1-i)z_p - \tanh[(1-i)z_p]}. \quad (3.30)$$

Here we have introduced the symbol z_p to denote the ratio of the particle radius to the thermal penetration depth into the particle, namely

$$z_p = (\omega a^2 / 2\kappa_p)^{1/2}. \quad (3.31)$$

Similarly, we find that \bar{p}'_p is given by

$$\bar{p}'_p = -\frac{3p'_s}{b_i^2 G(b_i)} + i(\gamma_p - 1) \frac{\rho_{p0} c_{pp}}{\beta_p T_0} \frac{\omega \kappa_p}{c_{sp}^2} \left[\frac{3}{b_i^2 G(b_i)} - \frac{3}{q_i^2 G(q_i)} \right] \bar{T}'_s, \quad (3.32)$$

where $G(b_i)$ is real and is given by

$$G(b_i) = \frac{j_0(b_i)}{b_i j'_0(b_i)} = \frac{\tan(b_i)}{b_i - \tan(b_i)}. \quad (3.33)$$

This function has an infinite number of zeros, each associated with an acoustic resonance within the particle (for a more complete study of acoustic resonances in an ideal fluid sphere see Überall *et al.* 1979).

Returning to (3.32) we see that \bar{p}'_p depends on both the temperature and the pressure at the surface of the particle. However, the temperature comes in only through a factor that is of the order $\omega \kappa_p / c_{sp}^2$ relative to the surface-pressure term, and may therefore be neglected. Thus,

$$\bar{p}'_p = -\frac{3}{b_i^2 G(b_i)} p'_s. \quad (3.34)$$

Because of the singular behaviour of $G(b_i)$, the pressure is seen to become infinity at those values of b_i that correspond to acoustic resonances within the particle. These owe their existence to our neglect of viscosity, and of the second term in (3.32). The lowest root occurs at $b_i = \frac{1}{2}\pi$, well beyond the resonance due to volume pulsations. Below such values, \bar{T}'_p and \bar{p}'_p are valid representations of the temperature and pressure variations within the particle. Beyond them, that interpretation is not

meaningful. However, \bar{T}'_p and \bar{p}'_p retain their mathematical meaning. The issue will be re-examined later, where it is shown that \bar{T}'_p differs little from T'_s for values of z_p as large as 1, and that \bar{p}'_p differs little from p'_s for values of b_i also as large as 1.

Returning now to (3.22) and (3.26), we eliminate T'_s and p'_s in favour of \bar{T}'_p and \bar{p}'_p , and introduce the non-dimensional variables

$$T = \frac{\bar{T}'_p}{\Theta'_f} \quad \text{and} \quad \Pi = \frac{\bar{p}'_p}{P'_f} \quad (3.35a,b)$$

to write those equations as

$$\begin{aligned} -i(\gamma_f - 1)b^2[(\kappa_f/\kappa_p)(q - b)G(q_i) + i\beta_p/\beta_f]T - [\gamma_p b^2 N_s + (1 - ib)b_i^2 G(b_i)]\Pi \\ = 3(1 - ib) + 3i(\gamma_f - 1)(b/q)^2(q - b). \end{aligned} \quad (3.36)$$

and

$$[(1 - iq)q_i^2 G(q_i)/3 + ihz^2]T + [(1 - ib)b_i^2 G(b_i)/3 - 2i(\beta_p/\beta_f)z^2/3]\Pi = -2 + i(q + b), \quad (3.37)$$

where $h = 2\rho_{p0}c_{pp}/3\rho_{f0}c_{pf}$, and where

$$z = (\omega a^2/2\kappa_f)^{1/2} \quad (3.38)$$

is the ratio of particle radius to thermal penetration depth into the external fluid and related to z_p by means of $z = z_p(\kappa_p/\kappa_f)^{1/2}$. Before obtaining general results from these equations, we consider them in some limiting cases that provide a basis for comparison.

3.1. Nearly-rigid particles

This case applies closely to droplets in gases because of the very small compressibility of the droplets relative to that of the gas outside, as well as to solid particles in either gases or liquids. Here $\beta_p/\beta_f \rightarrow 0$, and $N_s \rightarrow 0$, so that (3.36) and (3.37) give

$$T = \frac{i}{hz^2} F, \quad (3.39)$$

where F is a complex function of both z and z_p , and is given by

$$F = \frac{1}{1 + z - iz} + \frac{k_f}{k_p} G(q_i), \quad (3.40)$$

where $G(q_i)$ is defined in (3.30). Equation (3.39) was recently derived elsewhere (Temkin 1998). When both z and z_p are very small, we obtain from (3.39) the low-frequency limit,

$$T \approx 1 + ihz^2[1 + \frac{1}{5}(k_f/k_p)]. \quad (3.41)$$

3.2. Isothermal fluid

A second limit of interest occurs when the fluid outside the particle has a specific heat ratio which is nearly equal to unity. Here, the sound speed in the fluid is very nearly equal to the isothermal value c_{Tf} , so that (3.36) gives

$$\Pi = -\frac{3(1 - i\omega a/c_{Tf})}{\gamma_p(\omega a/c_{Tf})^2 N_T + b_i^2 G(b_i) - ib_i^2 G(b_i)\omega a/c_{Tf}}, \quad (3.42)$$

where $N_T = \rho_{f0}c_{Tf}^2/\rho_{p0}c_{Tp}^2$. When the particle is much smaller than the wavelength, $b_i \ll 1$ and $b_i^2 G'(b_i) = -3$, so that (3.42) becomes

$$\Pi = \frac{1 - i\omega a/c_{Tf}}{1 - (\omega/\omega_{T0})^2 - i(\omega a/c_{Tf})}, \quad (3.43)$$

where

$$\omega_{T0} = \frac{c_{Tp}}{a} (3\rho_{p0}/\rho_{f0})^{1/2} \quad (3.44)$$

is the particle's lowest resonant frequency for volume pulsations when the temperature of the fluid outside remains constant. We shall refer to this as the isothermal resonance frequency, noting that the temperature in the particle generally varies, as shown by (3.37).

3.3. Non-conducting fluid

We now consider the limiting case when the thermal conductivity of the external fluid vanishes. This is obtained by letting $z \rightarrow \infty$ in the above results. Thus, (3.37) gives

$$\Pi = T/\xi, \quad (3.45)$$

where

$$\xi = \frac{\beta_p \rho_{f0} c_{pf}}{\beta_f \rho_{p0} c_{pp}}. \quad (3.46)$$

Substituting this into (3.37) and using the thermodynamic relation $\beta^2 T_0 c_s^2 = c_p(\gamma - 1)$, gives

$$T = \frac{3(1 - ib)\xi}{(1 - ib)b_i^2 G(b_i) + b^2 N_s}. \quad (3.47)$$

Again, when b_i is small, this reduces to the well-known result

$$T = \frac{(1 - ib)\xi}{1 - \omega^2/\omega_{s0}^2 - ib}, \quad (3.48)$$

where $\omega_{s0}^2 = \gamma_p \omega_{T0}^2$ is the adiabatic value of the natural frequency for radial oscillations. The corresponding result for the pressure is then given by (3.43), with c_{sf} and ω_{s0} instead of the isothermal values appearing there. It is noted that the adiabatic limit predicts a temperature discontinuity across the interface equal to

$$\Theta'_f - \bar{T}'_p = (1 - \xi)\Theta'_f. \quad (3.49)$$

3.4. Low-frequency limit

Finally, we consider the very low-frequency limit of the complete results. Here $b \ll 1$, $b_i \ll 1$, and both z and z_p are small. Thus, using (3.36) and (3.37), we obtain the leading-order results

$$T \approx 1 + ihz^2 [1 - \xi + \frac{1}{3}(k_f/k_p)] \quad (3.50)$$

and

$$\Pi = 1 + \frac{1}{3}\gamma_p N_s b^2 [1 + \rho_{p0}/5\rho_{f0} - (\gamma_p - 1)/\gamma_p \xi]. \quad (3.51)$$

The first differs from the equivalent limit for a rigid particle, (3.14), only in that it contains the quantity ξ inside the square bracket. The second shows that the pressure

in the particle remains essentially equal to that outside over a wide range of small frequencies. In the case of a gas bubble in a liquid, ξ , N_s , and ρ_{f0}/ρ_{p0} are of the order of 10^3 or larger, so that (3.51) gives

$$\Pi \approx 1 + (\omega/\omega_{T0})^2, \quad (3.52)$$

where we also used (3.44).

4. General results

We now consider the general case when both fluids can have arbitrary values of the thermal expansion, specific heat ratio, compressibility and heat conductivity. This case requires the solution of the complete equations for T and Π . This solution can be obtained without difficulty, but the resulting expressions are too cumbersome to be useful. Instead of presenting those expressions here, we write the solution for the temperature in the symbolic form

$$T = \frac{X + iY}{U + iV}, \quad (4.1)$$

where the functions X , Y , U and V are real and are given in Appendix A. The pressure ratio, Π , can be obtained by using (4.1) in (3.36) or (3.37).

Although algebraically involved, those expressions are exact within the model and describe the basic physics of the problem in terms of the physical properties of the two fluids and the frequency. The expressions can be used to evaluate the real and imaginary parts of Π and T , and the corresponding surface values, Π_s and T_s , respectively, obtained from Π and T by means of (3.29) and (3.34), respectively. The results apply to bubbles and droplets in liquids, as well as to droplets in gases.

Below, we consider droplets and bubbles in liquids. Because the results are strongly dependent on the properties of the fluids, it is the best to consider those cases separately. For simplicity, we take, in both cases, a particle having a diameter equal to 100 microns. Similar results are obtained for other diameters. Finally, all results will be shown for frequencies such that the small parameter ratio $k^2/|K|^2 = 2\omega\kappa_f/c_{sf}^2$ is smaller than 10^{-2} for both fluids, and for values of $b = \omega a/c_{sf}$ smaller than 1.

4.1. Gas bubble in a liquid

We first show the average and the surface values of the non-dimensional temperature and pressure. Those values are, of course, not identical, except at low frequencies. As the frequency increases, differences appear owing to the first spatial variations with the bubble. Figure 2 shows the average and surface values of the magnitude of the temperature versus $z_p = (\omega a^2/2\kappa_p)^{1/2}$. It is seen that there are no differences for values of z_p as large as 1. Beyond this value some differences appear, as anticipated by our order of magnitude estimates in §2, because of the increasingly smaller penetration of the thermal waves into the bubble.

Figure 3 shows the pressure ratios versus b_i . It is seen that the surface and average pressure ratios agree closely for values of b_i as large as 1. Beyond this value the curves separate, with the surface pressure magnitude showing wide oscillations that include acoustics resonances within the particle.

In figure 4 we show the magnitude of Π as a function of the non-dimensional frequency, ω/ω_{T0} , as predicted by the present theory. For comparison we also show the bubble pressure as calculated by the isothermal and the non-conducting fluids theories. It is seen that the isothermal-fluid model agrees with the present theory over a frequency range that extends, for a bubble of this size, to about ten times larger

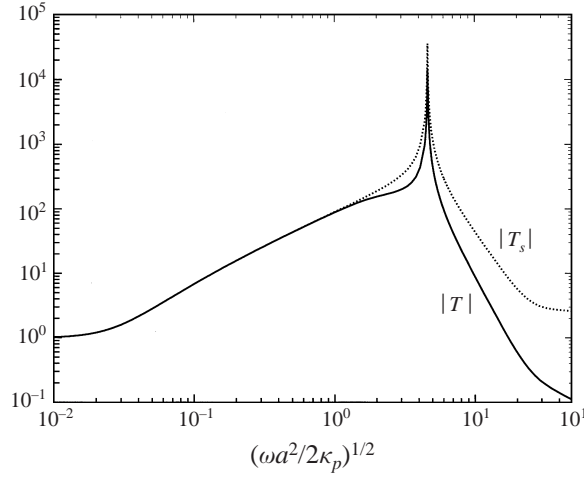


FIGURE 2. Amplitudes of the average particle temperature ratio, $T = \bar{T}'_p/\Theta'_f$ (—), and the surface temperature ratio, $T_s = T'_s/\Theta'_f$ (.....), for a 100 μm diameter air bubble in water vs. z_p .

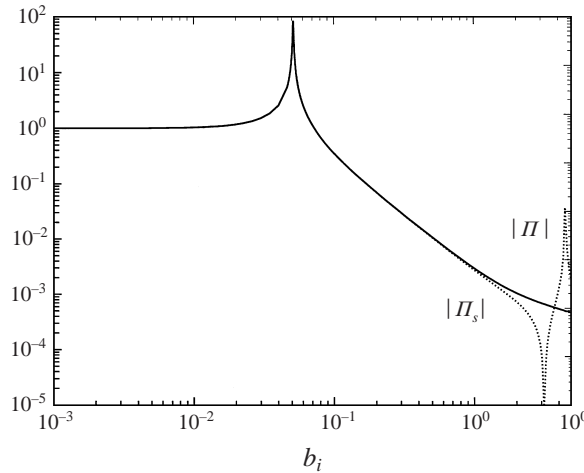


FIGURE 3. Amplitudes of the average particle pressure ratio $\Pi = \bar{p}'_p/P'_f$ (—), and the surface pressure ratio, $\Pi_s = p'_s/P'_f$ (.....), for a 100 μm diameter air bubble in water vs. $\omega a/c_{sp}$.

than ω_{T0} . Beyond that value, the isothermal pressure amplitude decreases faster than the more complete theory predicts. The figure also shows that the adiabatic model agrees with the general results for frequencies below resonance. At frequencies larger than that, it predicts amplitudes that over- or underestimate the actual response. In addition, of course, the adiabatic pressure peaks at a different frequency.

4.1.1. Comparison to other results

The results obtained above may be compared to the small-amplitude results of Prosperetti (1991). For simplicity, we consider the ratio of bubble temperature to bubble pressure. This ratio is explicitly given by (3.22) of Prosperetti's paper, and appears in other important aspects of the theory. In the present notation, that equation

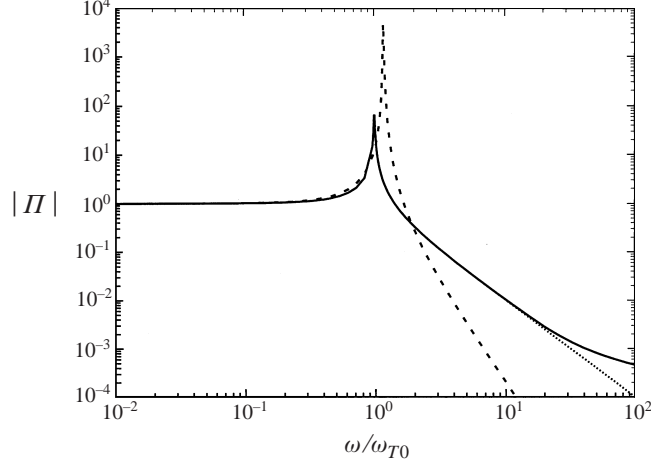


FIGURE 4. Amplitudes of the average pressure ratio for a 100 μm diameter air bubble in water vs. ω/ω_{T0} : \cdots , $\gamma_f - 1 \approx 0$; $---$, $k_f = 0$; $—$, general results.

can be expressed as

$$\frac{\tau_P}{\Pi_P} = \xi \left[1 - \frac{\sinh(q_i y)}{y \sinh(q_i)} \right], \quad (4.2)$$

where $y = r/a$, and where the suffix P has been added to identify the result. To compare with our T/Π , we need the spatial average of (4.2). This is obtained using the prescription given by (3.18) for the density, and is given by

$$\frac{\bar{\tau}_P}{\Pi_P} = \xi [1 + 3/q_i^2 G(q_i)], \quad (4.3)$$

where $G(q_i)$ is given by (3.30). In the limit of small frequencies, $q_i^2 G(q_i) \approx -3 + \frac{2}{5} i z_p^2$, so that $\bar{\tau}_P/\Pi_P \rightarrow 0$ as $\omega \rightarrow 0$. This is consistent with Prosperetti's boundary condition, and differs from our results which give $T/\Pi \rightarrow 1$ in the same limit.

We also include in our comparisons a third theory, obtained in Appendix B. This retains the temperature fluctuations in the liquid, but neglects the pressure disturbance there. That theory gives

$$\frac{\bar{\tau}_u}{\Pi_u} = \xi + \frac{1 - \xi}{h z^2} \frac{i}{F} + \frac{1}{h z^2} \frac{i}{F} \frac{1 - \Pi_u}{\Pi_u}. \quad (4.4)$$

To compare this with T/Π and $\bar{\tau}_P/\Pi_P$, we need Π_u , the pressure in the bubble that applies when the pressure disturbance in the liquid is neglected. This quantity is not given by the simple analysis of Appendix B. However, if we make the additional assumption that $\Pi_u \approx 1$ at all frequencies, then

$$\frac{\bar{\tau}_u}{\Pi_u} = \xi - \frac{3(1 - \xi)}{q_i^2} \frac{k_p/k_f}{\left[1 + z - iz + \frac{k_f}{k_p} G(q_i) \right]^{-1}}, \quad (4.5)$$

where, for the purpose of comparison we have left the symbol Π_u on the left-hand side, even though it has been taken to be equal to unity. Thus, (4.5) applies provided the pressure in the particle is equal to that of the fluid at all frequencies. For simplicity, we refer to this result as the *uniform-pressure* theory.

Because of the large value of ξ applicable to gas bubbles in water, (4.3) differs

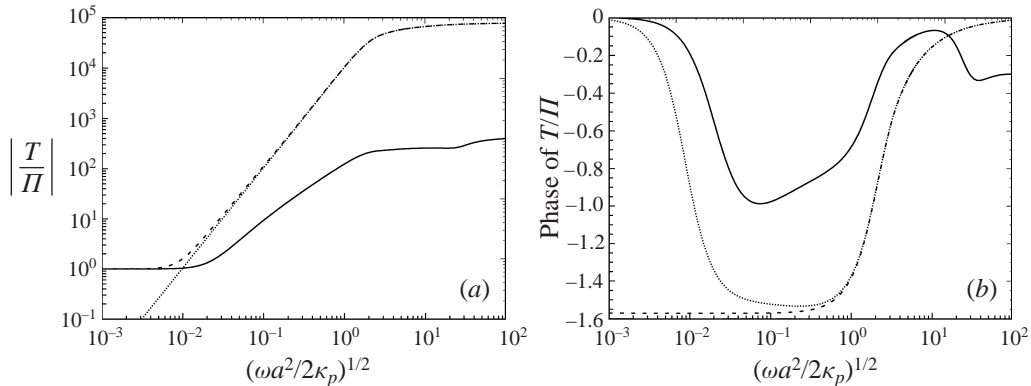


FIGURE 5. (a) Amplitude and (b) phase of T/Π for a 100 μm diameter air bubble in water vs. z_p : \cdots , equation (4.3); $---$, equation (4.4); $---$, general results.

from (4.5) only in that the quantity $1/(1+z-iz)$ is absent in it. This quantity takes into account the temperature variations in the liquid outside the bubble, which are neglected in Prosperetti's analysis, and is significant only at low frequencies, as shown below. Thus, it appears that $\bar{\tau}_p/\Pi_p$ is, at all frequencies but the lowest, equal to $\bar{\tau}_u$.

In figures 5(a) and 5(b) we show a comparison of the magnitude and phase angles of the average temperature–pressure ratio as predicted by these three different theories. It is seen that the uniform-pressure theory agrees with the more complete results derived here at the lowest frequencies. This occurs because both sets retain the temperature fluctuations in the liquid, and because in the limit of low frequencies, the pressure disturbance, which is retained in the more complete analysis, is negligible. On the other hand, it is seen that beyond the lowest frequencies shown in those figures, the uniform-pressure theory agrees very closely with Prosperetti's theory, implicitly indicating that the effects of the pressure disturbance are not taken into account in Prosperetti's model.

However, the more complete theory, though initially agreeing with the uniform-pressure results, departs significantly from them, and from Prosperetti's, as the frequency increases, being more than two orders of magnitude lower than either of them in the range $1 \leq z_p \leq 10^2$. Such large differences are due to the neglect, in those theories, of the pressure disturbance in the liquid. Unlike the fluid temperature fluctuation, where a frequency region exists that makes its neglect reasonable, the pressure disturbance cannot generally be neglected. This may be seen by considering the linearized momentum equations for both fluid in the particle and outside it. Thus, in the absence of viscosity and for monochromatic time dependence, we have, from (2.4), $i\omega\rho_{p0}\mathbf{u}_p = \nabla p'_p$ for the particle, and $i\omega\rho_{f0}\mathbf{u}_f = \nabla p'_f$ for the exterior fluid. Taking the dot product of these with the unit normal vector at the bubble surface and applying the boundary condition on the velocity, we obtain, since P'_f is independent of position,

$$\left(\frac{\partial p'_p}{\partial r}\right)_{r=a} = \frac{\rho_{p0}}{\rho_{f0}} \left(\frac{\partial \tau'_f}{\partial r}\right)_{r=a}. \quad (4.6)$$

The length scale for changes of pressure in either fluid is the corresponding acoustic wavelength. Hence, we have, in analogy with the temperature estimate in §2,

$$|p'_s - p'_p| \approx \frac{\rho_{p0}c_{sp}}{\rho_{f0}c_{sf}} |p'_s - P'_f|. \quad (4.7)$$

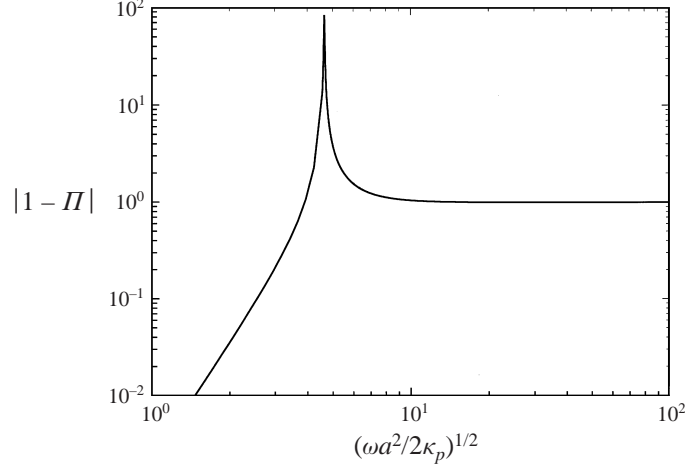


FIGURE 6. Amplitudes of the pressure-disturbance ratio for a 100 μm diameter air bubble in water vs. z_p .

Given the very small value of $\rho_{p0}c_{sp}/\rho_{f0}c_{sf}$ for gas bubbles in water, (4.7) shows that the pressure inside the bubble is nearly uniform, as we already know. But by the same equation, the pressure changes in the exterior fluid are not negligible, and produce, as figure 5 shows, significant differences in the field within the particle. This is further shown in figure 6, where the magnitude of the pressure disturbance at the surface of the bubble is displayed as a function of z_p . Thus, we see that beginning at about $z_p = 1$, the magnitude of the pressure disturbance at the surface of the particle increases rapidly, becoming quite large at resonance and beyond.

4.1.2. Polytropic index

Because of their near uniformity in the bubble, it is sometimes assumed that the pressure and the temperature are, at every instant, related by an equation of the form $T_p = c p_p^{(\kappa-1)/\kappa}$, where κ is called the polytropic index. Of course, this index depends on the properties of both fluids as well as on the frequency. It therefore does not represent a property of the gas in the bubble, as implied by its name. Nevertheless, the relation has proved to be useful in some contexts, and it is therefore appropriate to include it here, even though, as figure 2 shows, the temperature non-uniformity is significant for values of z_p equal to 1 or larger. Adapted to the small-amplitude oscillation being considered, the polytropic relationship can be written as

$$T = \frac{\gamma_p}{\gamma_p - 1} \frac{\kappa - 1}{\kappa} \xi \Pi. \quad (4.8)$$

Because the temperature and pressure ratios generally have different phases, this equation implies that the polytropic index κ is complex. Its value can be obtained in terms of the complex ratio T/Π , of $\bar{\tau}_p/\Pi_p$ in Prosperetti's theory, or of the equivalent ratio for the uniform-pressure theory, $\bar{\tau}_u/\Pi_u$. Thus, for example, for the present theory we have

$$\kappa = \left[1 - \frac{\gamma_p - 1}{\gamma_p \xi} \frac{T}{\Pi} \right]^{-1}. \quad (4.9)$$

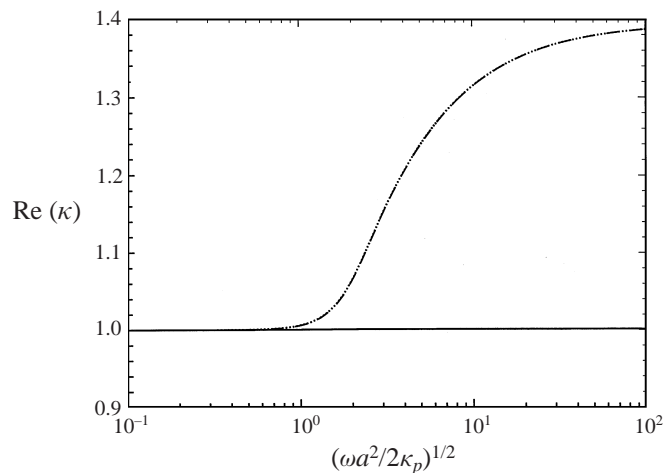


FIGURE 7. Real part of κ for a 100 μm diameter air droplet in water vs. z_p : \cdots , uniform-pressure theory; $---$, Prosperetti; $—$ present results.

The existence of an imaginary part in this expression indicates that the pulsations are accompanied by dissipation, and in fact, as shown later, the imaginary part of κ is directly associated with the thermal damping of a pulsating bubble. Because of that connection, we postpone the discussion of the imaginary part of κ until section (§8). In figure 7 we give the real part of κ as predicted by the three separate theories mentioned above. It is seen that the uniform-pressure theory predicts a real part of κ that is in agreement with Prosperetti's results, whereas the more complete theory differs, significantly, from both as the frequency increases. In particular, it is seen that the real part of κ , as given by (4.9), is essentially equal to 1 in the range of validity of the theory. The reason for this is that the pressure disturbance effectively maintains the pressure in the bubble at the same value as the pressure in the liquid, except near resonance and beyond, where, however, the changes are such that T/Π remains approximately constant, as figure 5 *a* shows.

4.2. Droplet in a liquid

The response of a droplet to an acoustic wave in a liquid is, of course, very different from that of a gas bubble because the compressibility of the liquid in the drop is comparable to that of a fluid outside. However, for some droplets in some liquids, the droplets also magnify the driving field, although this time the magnification is not as marked. As we will show below, the small-amplitude peaks displayed by the curves occur near the natural isothermal frequency of oscillation. This frequency has a much higher value than that for a bubble of the same diameter because, here, the ratio of ambient densities appearing in (3.44), is about 1.

We begin by comparing the surface and average pressures and temperatures as we did for bubbles. In figures 8 (*a*) and 8 (*b*) we show the variations, with frequency, of those quantities for the case of toluene in water. Because the pressures change only by small amounts, we show their variation on a linear scale. The surface temperature, on the other hand, varies by several orders of magnitude, and is therefore shown on a logarithmic scale. It is noted that the differences between the average and surface values of the temperature ratios are rather significant for frequencies beyond $z_p = 1$.

Figure 9 (*a*) shows the pressure-fluctuation ratio predicted by the isothermal and the adiabatic theories, as well as the complete results predicted by (3.29). All three

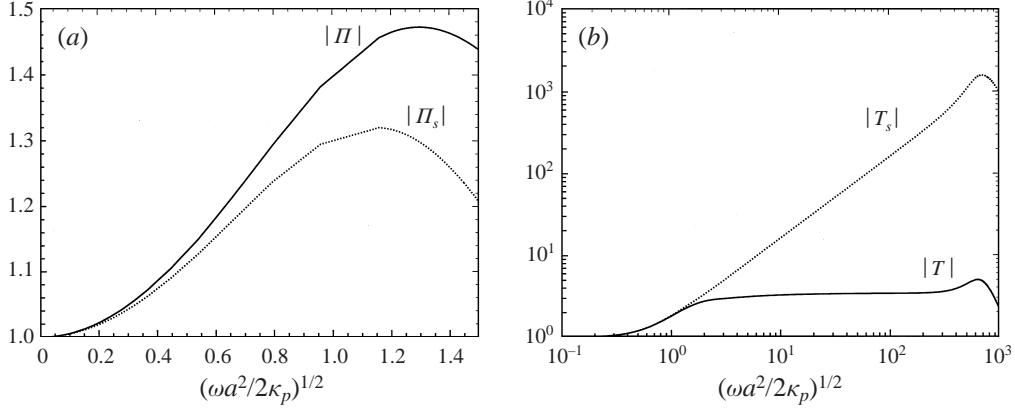


FIGURE 8. Amplitudes of (a) the pressure ratios and (b) the temperature ratios for a 100 μm diameter toluene droplet in water vs. z_p : \cdots , surface; — , average.

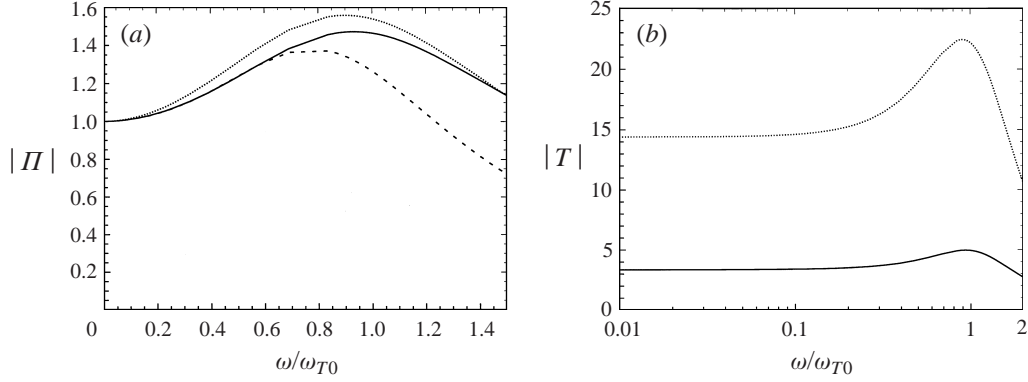


FIGURE 9. Amplitude of (a) the pressure ratio and (b) the temperature ratio for a 100 μm diameter toluene droplet in water vs. ω/ω_{T0} : \cdots , $k_f = 0$; — , general results. Dashed line in (a) is for the isothermal theory $\gamma_f - 1 \approx 0$.

theories predict a broad resonant response of small amplitude, but the amplitude and location of the maximum in those curves differ slightly among them. Finally, figure 9(b) shows the corresponding temperature-fluctuation ratio for the adiabatic and general models.

5. Heat transfer to the particle

The heat transfer rate, \dot{Q}_p , to the pulsating particle is given by (3.19), multiplied by the equilibrium surface area of the particle. Thus, using the thermodynamic relation $T_0\beta^2c_s^2 = c_p(\gamma - 1)$, we have, for the complex heat transfer rate

$$\dot{Q}_p = 4\pi ak_f[(1 - iq)(\Theta'_f - T'_s) + (1 - ib)(\beta_f T_0/\rho_{f0}c_{pf})(P'_f - p'_s)]. \quad (5.1)$$

This may be also expressed in real form by using $q = (1 + i)z$, and by noting that $\Theta'_f - T'_s$ and $P'_f - p'_s$ are equal to the differences of the absolute temperature and pressures between the fluid far from the particle and the particle's surface. Thus, if

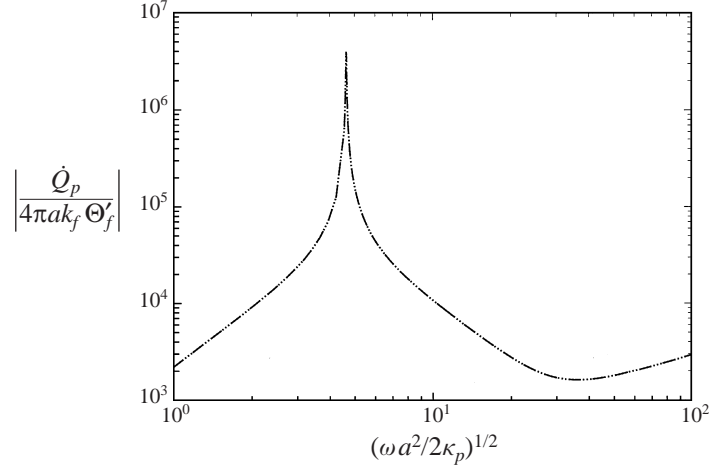


FIGURE 10. Amplitude of the non-dimensional heat flux, $|\dot{Q}_p/4\pi ak_f \Theta'_f|$, for a 100 μm diameter air bubble in water: \cdots , equation (5.2); $---$, equation (5.3).

\dot{Q}_p now denotes a real quantity, we obtain

$$\begin{aligned} \dot{Q}_p = & 4\pi ak_f(1+z)(T_f - T_s) - 2\pi a^2(\rho_{f0}c_{pf}k_f/\omega)^{1/2} \frac{d(T_f - T_s)}{dt} \\ & + 4\pi ak_f \beta_f T_0(p_f - p_s) + 4\pi a^2 \beta_f T_0 \frac{\kappa_f}{c_{sf}} \frac{d(p_f - p_s)}{dt}. \end{aligned} \quad (5.2)$$

This shows that, generally speaking, both temperature and pressure differences affect the heat transfer. However, as shown in figure 10 for air bubbles, the pressure dependence is negligible. In that figure we show the magnitude of $\dot{Q} = \dot{Q}_p/4\pi ak_f \Theta'_f$ as a function of z for a gas bubble, using (5.2) with and without the pressure term. It is seen that both results are essentially equal. The same is applicable for the phase $\dot{Q} = \dot{Q}_p/4\pi ak_f \Theta'_f$. Thus, with no appreciable error, the heat transfer rate is given by

$$\dot{Q}_p = -4\pi ak_f(1+z)(T_s - T_f) + 2\pi a^2(\rho_{f0}c_{pf}k_f/\omega)^{1/2} \frac{d(T_s - T_f)}{dt}. \quad (5.3)$$

Further simplification is possible when the average particle temperature can be used, but as shown in figures 2 and 9(b), this generally involves some error, particularly in the case of droplets in liquids. In the limit of low frequencies, however, (5.3) reduces to the well-known quasi-steady limit

$$\dot{Q}_p = -4\pi ak_f(\bar{T}_p - T_f). \quad (5.4)$$

6. Energy considerations

The results given in §5 may be used to obtain expressions for the rates at which energy is dissipated by mechanisms that remove energy from the incident wave. Those quantities are important in studies of sound propagation in suspensions, particularly in determining the attenuation of sound waves. They also can be used to determine damping coefficients for radially-pulsating gas bubbles. In the present study, the active mechanisms include acoustic radiation by the pulsating particle and thermal losses both in and outside the particle. Viscous losses, which exist in real fluids, have not

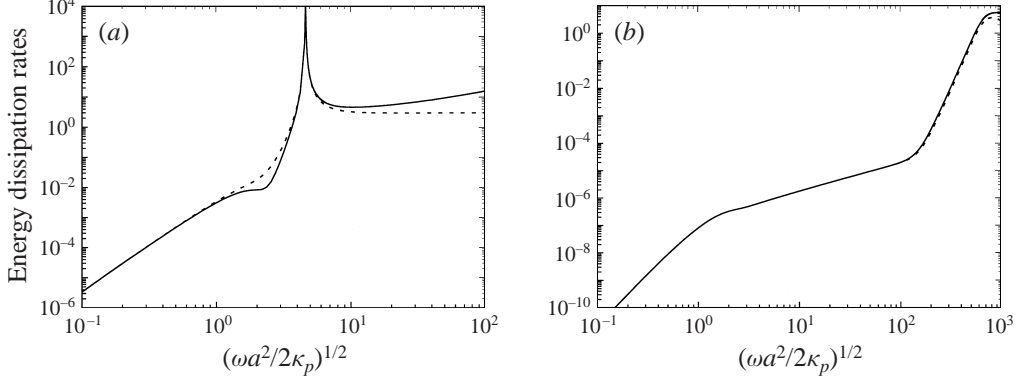


FIGURE 11. Energy dissipation rates: — input energy rate; ----, $\langle \dot{e}_{ac} \rangle + \langle \dot{e}_{th} \rangle$ for (a) an air bubble in water, and (b) a toluene droplet in water.

been included in the present analysis. As was pointed out earlier, viscous effects are small because the motions are purely radial. For translational motions, however, they are significant but in the linear approximation the related dissipation rate is decoupled from the pulsational dissipation rates, and may be calculated, separately, by taking the particles to be rigid, and by ignoring all thermal effects.

Now, for pulsational motions, on the other hand, the two dissipative mechanisms are generally coupled because the acoustic radiation is dictated by the pressure disturbance emitted by the particle, but this pressure disturbance is closely tied to the temperature field in the particle as we have seen earlier. To emphasize this, we first consider the total dissipation rate.

6.1. Total energy dissipation rate

When the pulsations are stationary, the total average energy dissipation rate, $\langle \dot{e}_{loss} \rangle_{total}$ is approximately equal to the average rate at which the external fluid does work on the particle, $\langle \dot{e}_m \rangle$. Thus, since the radial displacement per unit time is u_s , the surface velocity of the particle, we have

$$\langle \dot{e}_{loss} \rangle_{total} = -4\pi a^2 \langle \text{Re}(P_f) \text{Re}(u_s) \rangle. \quad (6.1)$$

Making use of (3.17) and (3.20), we express u_s as

$$u_s = (i\omega a/3)[\gamma_p \text{Im}(\Pi) - (\beta_p/\beta_f)(\gamma_f - 1) \text{Im}(T)/N_s](P_f'/\rho_{p0}c_{sp}^2). \quad (6.2)$$

Because the pulsations are monochromatic, we may express $\langle \text{Re}(P_f') \text{Re}(u_s) \rangle$ as $\frac{1}{2} \text{Re}(P_f' u_s^*)$, where u_s^* is the complex conjugate of u_s . Thus, substitution of (6.2) in (6.1) yields

$$\langle \dot{e}_{loss} \rangle_{total} = -\frac{2}{3} \pi a^2 c_{sf} b [\gamma_p \Pi - (\beta_p/\beta_f)(\gamma_f - 1) T/N_s] \frac{|P_f'|^2}{\rho_{f0} c_{sf}^2}. \quad (6.3)$$

This shows that the temperature and pressure in the particle determine the total energy loss. Of course, the corresponding contributions depend on the specific fluids being considered. For example, when the external fluid is a liquid, the second term is rather small, owing to the smallness of $(\gamma_f - 1)$. But even then, the effects of the temperature variations in the particle may be present through Π . In figure 11(a) we show this total dissipation rate for a 100 μm diameter air bubble in water, made

non-dimensional using $\frac{2}{3}\pi a^2 c_{sf} |P'_f|^2 / \rho_{f0} c_{sf}^2$. This quantity represents, essentially, an acoustic energy flux through an area equal to the equilibrium area of the particle. The figure shows the anticipated effects of resonance. The corresponding result for a droplet in a liquid is shown in figure 11 (b). The dashed lines shown in these figures are discussed below.

Now, because the only active mechanisms are acoustic radiation and thermal losses, the total dissipation rate is also equal to the sum of the corresponding dissipation rates, or

$$\langle \dot{e}_{loss} \rangle_{total} = \langle \dot{e}_{ac} \rangle + \langle \dot{e}_{th} \rangle. \quad (6.4)$$

It is however evident that the two quantities on the right-hand side of this equation cannot be identified with the corresponding terms in (6.2). Because in the literature it is customary to give results for the acoustic and thermal losses separately, we obtain those quantities below, noting that (6.4) provides a means for comparison of the results.

6.2. Acoustic radiation

We first compute the acoustic energy dissipation rate, $\langle \dot{e}_{ac} \rangle$. This is defined as the average energy that is radiated by the pulsating particle per unit time, in the form of acoustic waves. Since the motion is radial, all we need is the radial acoustic intensity,

$$I_r = \langle \pi'_f u_r \rangle, \quad (6.5)$$

where π'_f and u_r are the pressure and velocity produced by the sphere. These quantities are given by (3.3) and (3.4). We substitute those results into (6.5) and obtain

$$I_r = -\frac{1}{2} \rho_{f0} c_{sf} \operatorname{Re} [i|A|^2 k h_0^*(kr) h'_0(kr) + i|B|^2 K h_0^*(Kr) h'_0(Kr) + iA^* B K h_0^*(kr) h'_0(Kr) + iA B^* k h_0^*(Kr) h'_0(kr)], \quad (6.6)$$

where the asterisk represents a complex conjugate. The average energy lost due to acoustic radiation is equal to this intensity, multiplied by the area of any surface enclosing the sphere. For simplicity, we take a concentric spherical surface in the far field of the pulsating sphere, where the products of the spherical Bessel functions appearing in I_r can be approximated by their asymptotic values, giving

$$\langle \dot{e}_{ac} \rangle = 2\pi \rho_{f0} c_{sf} \{ |A|^2 + b|B|^2 / 4z \}, \quad (6.7)$$

where A and B are given by (3.15 a, b). Because of the smallness of $\omega \kappa / c_{sf}^2$, the second term in A may be neglected compared to the first. We may also neglect, entirely, the second term in (6.7). These simplifications yield

$$\langle \dot{e}_{ac} \rangle = 2\pi \rho_{f0} a^2 c_{sf} | \Pi - 1 |^2 \frac{|P'_f|^2}{\rho_{f0} c_{sf}^2}, \quad (6.8)$$

where $\Pi - 1$ is the non-dimensional pressure in the disturbance field.

6.3. Thermal dissipation

We now compute the average rate at which energy is lost due to thermal effects, $\langle \dot{e}_{th} \rangle$. This is due to dissipation in the particle $\langle \dot{e}_{th} \rangle_p$, and dissipation in the fluid outside, $\langle \dot{e}_{th} \rangle_f$. Both can be obtained from the well-known thermodynamic result that connects energy losses to the entropy increase. Thus, $\langle \dot{e}_{loss} \rangle = T_0 \langle \dot{S} \rangle$, where $\dot{S} = \int_V \rho (Ds/Dt) dv$ and s is the entropy per unit mass. (A more detailed description of the technique may

be found in Landau & Lifshitz 1959. Its application to the present problem is found in E & C, Fukumoto & Izuyama 1992, and Temkin 1993).

The entropy change in a volume V of fluid is due to a flow of heat into the volume, plus a contribution due to irreversibilities within the volume (see, for example, Temkin 1981). For an inviscid fluid, it can be expressed as

$$\dot{S} = k \int_A \mathbf{n} \cdot \frac{\nabla T}{T} dA + k \int_V \left(\frac{\nabla T}{T} \right)^2 dV, \quad (6.9)$$

where A is the surface area bounding the volume, and \mathbf{n} is a unit normal vector pointing away from it, and where we assumed that the thermal conductivity is constant. We now linearize this equation and then take the time average to obtain the thermal energy loss rate

$$\langle \dot{e}_{th} \rangle = -\frac{k}{T_0} \int_V \langle T' \nabla^2 T' \rangle dV. \quad (6.10)$$

The region of integration is naturally divided into the particle and the fluid outside. We consider each separately.

6.3.1. Particle

Using the energy equation for the particle, to express the Laplacian of the temperature, we have

$$\langle \dot{e}_{th} \rangle = \frac{1}{2} \omega \beta_p \text{Re} \left[i \int_{v_p} T_p p_p'^* dv \right]. \quad (6.11)$$

Now, since as we have seen that p_p' is very nearly uniform, it can be taken outside the integral and we obtain the simple result

$$\langle \dot{e}_{th} \rangle_p \approx \frac{2}{3} \pi a^2 c_{sf} b (\beta_p / \beta_f) (\gamma_f - 1) \text{Re}(iT\Pi^*) \frac{|P_f'|^2}{\rho_{f0} c_{sf}^2}. \quad (6.12)$$

When the spatial variations of T_p' and p_p' are used, we may express (6.11) as

$$\langle \dot{e}_{th} \rangle_p = 2\pi a^2 c_{sf} b (\beta_p / \beta_f) (\gamma_f - 1) \text{Re}(iI_p) \frac{|P_f'|^2}{\rho_{f0} c_{sf}^2}, \quad (6.13)$$

where

$$I_p = (a^3 \Theta_f' P_f'^*)^{-1} \int_0^a T_p' p_p'^* r^2 dr. \quad (6.14)$$

This is obtained in Appendix C. Using that result, we can write

$$\text{Re}(iI_p) = -\frac{1}{9} b_i^2 G(b_i) \text{Re}(iT\Pi^*) / j_0(b_i). \quad (6.15)$$

The thermal losses then follow from (6.13) and (6.15). However, as is shown below, the approximate result given by (6.12) is sufficient for all frequencies, except the highest.

6.3.2. Fluid

The computation of the thermal dissipation rate for the fluid follows the same lines as that for the particle, except that the fluid temperature fluctuation has two components: the background and disturbance fluctuations. Thus,

$$\langle \dot{e}_{th} \rangle_f = -\frac{k_f}{T_0} \Theta_f' \int_v \langle \nabla^2 \theta_f' \rangle dV - \frac{k_f}{T_0} \int_v \langle \theta_f' \nabla^2 \theta_f' \rangle dV. \quad (6.16)$$

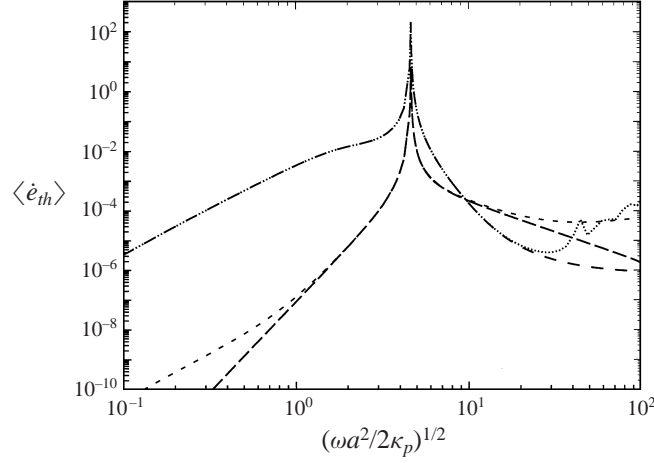


FIGURE 12. Non-dimensional thermal energy-dissipation rates for a 100 μm diameter air bubble in water: $\cdots\cdots$ particle, equation (6.13); $-\cdots-$, particle, equation (6.12); $----$, fluid, equation (6.18); $-\cdot-\cdot-$ fluid, equation (6.18) without $\kappa_f \dot{Q} / ac_{sf}$.

The first integral may be transformed into an integral over the area composed of the particle surface and a concentric spherical surface at infinity, where the disturbance is zero. The inner surface integral, multiplied by k_f , is equal to the particle heat transfer. The second integral can be simplified slightly by means of the energy equation for the fluid, (2.5). Thus, (6.16) becomes

$$\langle \dot{e}_{th} \rangle_f = \frac{1}{2T_0} \text{Re}(Q_p^* \Theta'_f) + \frac{1}{2} \omega \beta \text{Re} \left[i \int_{v_f} \theta'_f \pi'_f{}^* dV \right]. \quad (6.17)$$

This may be written as

$$\langle \dot{e}_{th} \rangle_f = 2\pi a^2 c_{sf} \{ b \text{Re}(iI_f) - (\kappa_f / ac_{sf}) \text{Re}(\dot{Q}) \} (\gamma_f - 1) \frac{|P'_f|^2}{\rho_{f0} c_{sf}^2}, \quad (6.18)$$

where $\dot{Q} = \dot{Q}_p / 4\pi a k_f \Theta'_f$ and

$$I_f = (a^3 \Theta'_f P'_f{}^*)^{-1} \int_a^\infty \theta'_f \pi'_f{}^* r^2 dr. \quad (6.19)$$

This integral is also considered in Appendix C and may be expressed as

$$I_f = \frac{(T_s - 1)(H_s^* - 1)}{q - b}. \quad (6.20)$$

It may be noted that the two quantities in the numerator of this equation are the temperature and pressure disturbance produced by the pulsating particles, evaluated at the surface of the particle. Ignoring these disturbances thus affects the thermal dissipation in the fluid. More importantly, however, the neglect of those disturbances affects the particle-dissipation rate, owing to the diminished ability of the particle to reduce its energy by sending excess energy into the fluid. This will be seen in the following figures where we show the dissipation rates, also made non-dimensional using $\frac{2}{3} \pi a^2 c_{sf} |P'_f|^2 / \rho_{f0} c_{sf}^2$. First, in figure 12 we display the particle and fluid thermal energy dissipation rates for a 100 μm diameter air bubble in water. Two results are shown in each case. For the particle, the first is based on (6.12) and ignores the

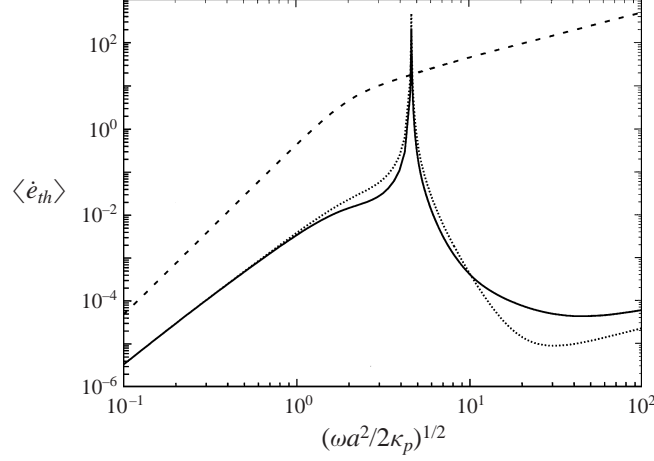


FIGURE 13. Non-dimensional total thermal energy-dissipation rates for a 100 μm diameter air bubble in water: —; equations (6.13) and (6.18) (without $\kappa_f \dot{Q} / ac_{sf}$); ·····, equation (6.22); ----, uniform-pressure theory, equation (6.23).

variations of pressure within the bubble. The second is obtained with the more accurate result given by (6.13). It is seen that the simpler result (6.12) agrees with the more accurate result for values of z_p that extend well above resonance.

For the thermal dissipation in the fluid, one dissipation rate is obtained from the complete result given by (6.18), and the other from the same equation without $(\kappa_f / ac_{sf}) \text{Re}(\dot{Q})$. It is seen that the fluid thermal energy dissipation rate is smaller than that in the particle at most frequencies, except the highest, where it becomes comparable to or even larger than that in the particle. At these frequencies, the thermal waves generated at the surface of the bubble barely penetrate into the fluid, but significant dissipation takes place in a thin layer around the bubble owing to the large thermal gradients there. However, at such frequencies the acoustic dissipation rate overwhelms the thermal dissipation. Hence, without significant loss of information, as far as the total energy-dissipation rate is concerned, the thermal dissipation rate may be computed by (6.12) for the particle, and by (6.18), without the second term inside the curly brackets, for the fluid.

Finally, we include here the thermal-energy dissipation rate that is obtained from the uniform-pressure theory derived in Appendix B. Here $\Pi_u = 1$ so that (6.12) yields

$$\langle \dot{e}_{th}^{unif} \rangle = \pi a^2 c_{sf} \frac{b}{z^2} (\gamma_f - 1) \xi |1 - \xi| \frac{|P_f'|^2}{\rho_{f0} c_{sf}^2} \text{Re} \left(\frac{1}{F} \right). \quad (6.21)$$

The thermal dissipation rates predicted by this equation and by the more complete results given by (6.12) and (6.18) are displayed in figure 13 for an air bubble in water. The salient feature in the graph is the strong discrepancy between the uniform-pressure thermal dissipation rate and the other two rates, both of which were obtained from a theory that allows the fluid outside the bubble to sustain both temperature fluctuations and temperature and pressure disturbances. The differences are clearly related to the neglect of the pressure disturbance, and produce two distinct effects. One is that the uniform-pressure theory does not display the effects of resonance that are apparent in the more complete theory. This is an anomaly because the larger amplitude at resonance must produce a larger dissipation rate. The second is the considerably larger dissipation that the uniform-pressure theory predicts at most frequencies. The

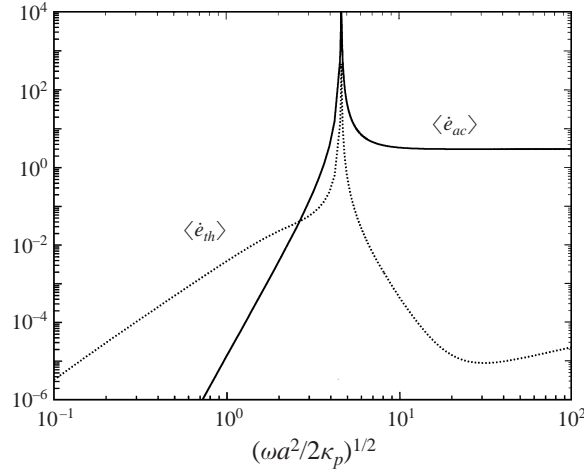


FIGURE 14. Non-dimensional energy-dissipation rates for a 100 μm diameter air bubble in water: —, acoustic; ·····, thermal (equation (6.22)).

main reason for this is that when $\Pi = 1$, the bubble is not able to release excess energy into the surrounding fluid via a mechanism that is *essentially reversible*, namely the pressure disturbance $\Pi - 1$. Were this mechanism not available, that energy would have to be dissipated within the bubble, thus increasing the damping.

In figure 14 we show the thermal and acoustic dissipation rates for an air bubble in water. It is seen that at all frequencies near resonance and beyond, the acoustic dissipation rate is the dominant loss mechanism.

Finally, the total energy dissipation rate for the same air bubble in water, as computed in terms of the sum of the two separately computed energy dissipation rates is shown in figure 11. As anticipated, the two computations give approximately the same results, except in a band of frequencies slightly below resonance, and at very high frequencies. The reasons for the differences are directly related to the differences between the surface and average temperature fields in the bubble, as shown in figure 2.

We now consider the energy-dissipation rates for a toluene droplet in water. To save space, we show in one graph, figure 15, both thermal and acoustic the dissipation rates. In this case, (6.18) has been used to calculate the thermal dissipation in the fluid. Although drastically different in shape, the same conclusions as found for the gas bubble apply here, namely the acoustic dissipation rate is dominant near resonance and beyond, and that the uniform-pressure theory overestimates the thermal dissipation rate, though not by as large a factor as it does for the gas bubble.

7. Attenuation in dilute suspensions

As the first application of the results obtained above, we consider the attenuation of plane sound waves in dilute suspensions. The derivation presented below is limited to situations where the resulting attenuation per wavelength is small. In that case, we may extract the attenuation from the energy dissipation rates by means of (see, for example, Landau & Lifshitz 1959) $\alpha = |\langle \dot{E}_{loss} \rangle| / 2c_{sf} E_0$, where \dot{E}_{loss} is the total energy loss per unit volume, and E_0 is the average acoustic energy in the incident wave that is contained in the same volume. For this case, the energy dissipation rates are additive, so that the energy loss produced by all the particles is equal to the number

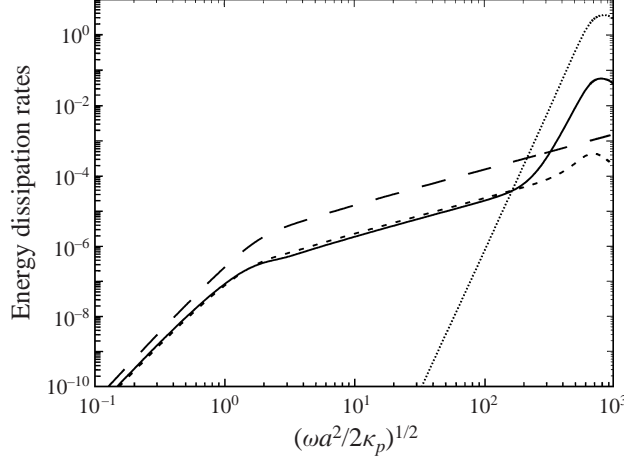


FIGURE 15. Non-dimensional energy-dissipation rates for a 100 μm diameter toluene droplet in water: \cdots , acoustic; — , thermal (equations (6.12) and (6.18)); --- , thermal, (equations (6.12) and (6.18) without $\kappa_f \dot{Q} / ac_{sf}$); $\text{-}\cdot\text{---}$, uniform-pressure theory (equation (6.21)).

of particles per unit volume, n , times the dissipation rate per particle. Further, the attenuations produced by each mechanism are separable, so that putting $\hat{\alpha} = \alpha c_{sf} / \omega$ we have $\hat{\alpha} = \hat{\alpha}_{ac} + \hat{\alpha}_{th}$, where

$$\hat{\alpha}_{ac} = n|\langle \dot{e}_{ac} \rangle| / 2\omega E_0 \quad \text{and} \quad \hat{\alpha}_{th} = n|\langle \dot{e}_{th} \rangle| / 2\omega E_0 \quad (7.1a,b)$$

are the non-dimensional acoustic and thermal attenuations. In addition to these, a particle in a sound wave will also produce sound attenuation owing to its lateral motion in the wave. The latter attenuation, called viscous in the literature, has also been considered before by many investigators, and the author has recently presented a theory for it that covers a very wide range of frequencies (Temkin 1996, 1998).

Now, the reference energy, E_0 , for a plane wave is given by $E_0 = |P_f'|^2 / 2\rho_f c_{sf}^2$. Thus, we immediately obtain

$$\hat{\alpha}_{ac} = \frac{3}{2} \phi_v |\Pi - 1|^2, \quad (7.2)$$

where $\phi_v = \frac{4}{3} n \pi a^3$ is the particle volume fraction in the suspension.

The thermal attenuation coefficient may be expressed in various forms, depending which of the thermal dissipation rates is used. The most detailed description is provided by (6.13) and (6.18) which yield

$$\hat{\alpha}_{th} = \frac{3}{2} \phi_v (\gamma_f - 1) |(\beta_p / \beta_f) \text{Re}(iI_p) + \text{Re}(iI_f) - \text{Re}(\dot{Q}) / 2z^2|. \quad (7.3)$$

A simpler form, adequate for most frequencies is obtained by neglecting the last term in the above equation, and by using (6.12) for the thermal dissipation rate in the particle. Thus,

$$\hat{\alpha}_{th} = \frac{3}{2} \phi_v (\gamma_f - 1) |(\beta_p / \beta_f) \text{Re}(iT\Pi^*) + \text{Re}(iI_f)|. \quad (7.4)$$

This equation can also be used for the uniform-pressure theory simply by removing the last term, and by taking the pressure ratio equal to 1, or by using (6.21) in the definition of the thermal attenuation. Thus,

$$\hat{\alpha}_{th}^{unif} = \frac{3}{4z^2} \phi_v (\gamma_f - 1) \xi |1 - \xi| \text{Re}\left(\frac{1}{F}\right). \quad (7.5)$$

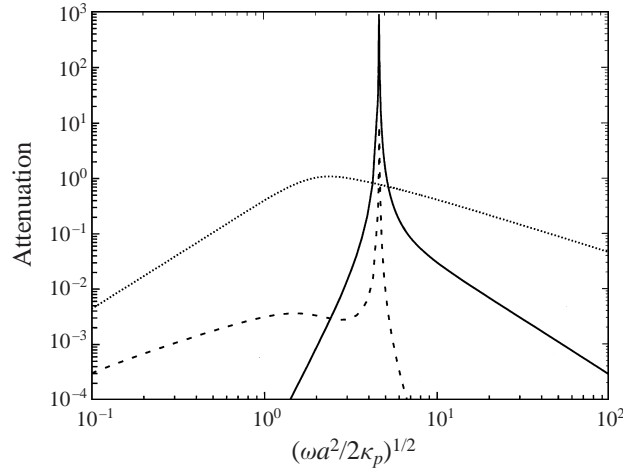


FIGURE 16. Non-dimensional attenuation for a dilute bubbly liquid of air bubbles in water, $\phi_v = 10^{-3}$: —, acoustic; ·····, thermal, uniform-pressure theory; ----, thermal.

These above coefficients apply to the three types of fluid combinations under consideration. We consider each case separately.

7.1. Bubbly liquids

As is well known, a very small concentration of bubbles produces a very large attenuation in the vicinity of resonance. This occurs mainly as a result of the much larger compressibility of the bubbles relative to the liquid. The ratio between the two, called N_s in this work, multiplies the volume concentration in an explicit expression for the acoustic attenuation, thereby magnifying its effects by a large factor. In figure 16 we show the non-dimensional attenuation for a bubbly liquid consisting of 100 μm diameter air bubbles in water, and having a concentration equal to 10^{-3} . Although this is indeed small, the peak value of the attenuation exceeds unity by a large factor. Thus, the energy estimate given above is not applicable in the vicinity of resonance. In such cases, a second-order estimate, still limited to dilute suspensions, may be obtained by other means, for example the Kramers–Kronig equations, as done recently by the author (Temkin 1990) for an isothermal suspension, but this is beyond the scope of the present work. Figure 16 also shows the thermal attenuation coefficient that is predicted by the uniform-pressure theory. As it is seen, this overestimates the thermal attenuation by a large amount, except at resonance, where it underestimates it.

7.2. Liquid-droplet aerosols and emulsions

These cases are related because the particles in them are droplets. There are, however, significant differences between the two, both in magnitude and trend. Also, long-standing theories exist for both cases, and it is important to compare our results with them. Notable among them is the theory of Epstein & Carhart, who considered thermal and viscous attenuation in suspensions and emulsions (E & C). In the present notation, their thermal attenuation may be expressed as

$$\hat{\alpha}_{th} = \frac{3}{4z^2} \phi_v (\gamma_f - 1) (1 - \xi)^2 \operatorname{Re} \left(\frac{1}{F} \right), \quad (7.6)$$

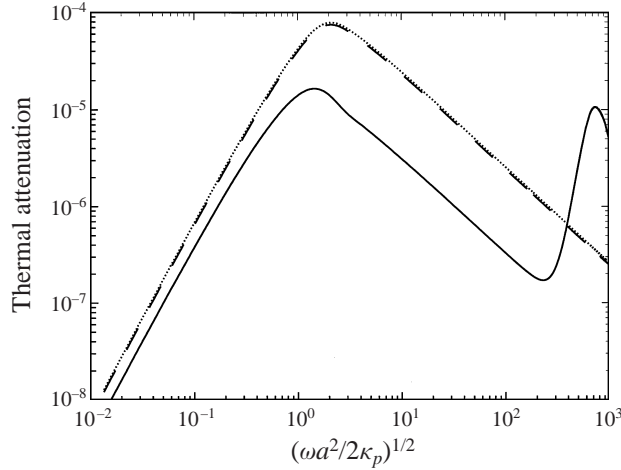


FIGURE 17. Non-dimensional thermal attenuations for a dilute emulsion of $100\ \mu\text{m}$ diameter toluene droplets in water, $\phi_v = 10^{-3}$: — — —, uniform-pressure theory; — — —, present results; ····, E & C.

where the complex function F is given by (3.40). As pointed out by Allegra & Hawley (1972), this result had been obtained earlier by Isakovich (1948). Both results apply when the particle diameter is smaller than the wavelength in the incident wave, and are therefore directly comparable to ours.

First we consider the case of droplets in gases. In this aerosol, the ratio of particle to fluid compressibilities is very small, so that over a wide range of frequencies the particles can be considered rigid. The thermal attenuation for them may be obtained from the thermal dissipation rates given earlier by taking the limit $\beta_p/\beta_f \rightarrow 0$. Thus,

$$\hat{\alpha}_{th}^{rigid} = \frac{3}{4z^2} \phi_v (\gamma_f - 1) \text{Re} \left(\frac{1}{F} \right). \quad (7.7)$$

Although expressed differently, this result is equal to one derived recently by the author from a new theory for sound propagation in suspensions of rigid particles (Temkin 1998), as may be seen from equations (A 8) and (43 b) of that work. Now, for liquid droplets in gases, the quantity ξ appearing in (7.6) is typically smaller than 0.01 and can therefore be neglected. Thus, the rigid-particle theory agrees, in this case, with that of E & C. It also agrees with the particulate-relaxation theory (Temkin & Dobbins 1966a), and has been verified experimentally for both solid particle aerosols (Zink & Delsasso 1958), and liquid particle aerosols (Temkin & Dobbins 1966b).

We now consider emulsions. Here ξ is of order 1, and must therefore be retained in the results. As its definition shows, this quantity contains the ratios of thermal expansions and heat capacities. In the theory presented here, these ratios play different roles at different frequencies, and it is only in the limit of low frequencies that ξ appears as a separate group. Thus, for example, in the limit of low frequencies, our thermal attenuation is proportional to $(1 - \xi)[1 - \xi + \frac{1}{5}(k_f/k_p)]$. On the other hand, in the theory of Isakovich and of E & C, ξ appears only as indicated explicitly in (7.6). Since the function F in that equation does not contain the thermal expansion coefficients or the heat capacities of either fluid or particle, we find the surprising result that those theories differ from the rigid-particle result only by a constant factor at all frequencies. We also find that significant differences exist between the E & C result and ours, as shown figure 17, where we compare our thermal attenuation result,

(7.3), to that of E & C for an emulsion of $100\ \mu\text{m}$ toluene droplets in water having a volume concentration equal to 10^{-3} . The reason for the differences can be traced to the absence of a pressure disturbance in (7.6). This follows from comparison between the attenuation predicted by the uniform-pressure theory, also shown in the figure, and the other results. It should be added that these differences occur for $b < 1$, that is, in the long-wavelength frequency range.

The agreement between the E & C and uniform-pressure theories seems to imply that the pressure disturbance was not considered by E & C. But this implication is not warranted, as their derivation clearly shows. The reasons for that agreement are made clear in their Appendix A, where it is made evident that the explicit results they give apply *only* to droplets in gases, as is also clear in title of their paper. Thus, (7.6) does not apply to emulsions. This fact was known to Allegra & Hawley who re-examined the attenuation theory of E & C very closely, and extended it so as to include solid elastic particles, claiming that E & C obtain the correct result only fortuitously. But in the case of thermal attenuation in emulsions, Allegra & Hawley obtain the same long-wavelength result given earlier by E & C and by Isakovich. That result is contained in their coefficient A_0 given by their equation (10). This is then approximated to obtain their equation (13), from which (7.6) follows, but the magnitude of the errors introduced by the multiple approximations made in the process is unclear.

A related issue is the attenuation of the main wave produced by pulsations of the particles. Allegra & Hawley do mention scattering, and in fact their equation (32) gives the lowest-order scattering coefficient. That equation consists of two terms. The first is related to our low-frequency disturbance pressure, and the second is due to the scattering that is produced by a particle executing translational oscillations. But it is unclear whether the related attenuation effect was included in their general solution for the attenuation at all frequencies. That attenuation is not explicitly mentioned in the text, nor do their figures for emulsions give an indication of acoustic radiation influencing the attenuation, although this could be due to the small size of the particles used by them when reducing the theory. E & C do not mention the acoustic attenuation either, but this is not surprising, given that the paper refers to droplets in gases.

Now, although droplets do not pulsate as readily as bubbles, the energy they radiate is, at some frequencies, comparable to or larger than to the energy losses associated with thermal losses. This is shown in figure 18 for a dilute emulsion composed of toluene droplets in water. Also shown in the figure is the attenuation coefficient that applies to an emulsion as a result of viscous and mechanical scattering effects that are active owing to the translational motion of the droplets. The viscous attenuation component has been calculated by several investigators in the past (for example, Epstein 1941; Urlick, 1948; E & C; Allegra & Hawley 1972), but as we have shown recently using two different approaches (Temkin 1996, 1998), their results do not correctly describe the dependence of that attenuation on the ratio between fluid and particle densities. The net effect of the differences is to increase the magnitude of the translational motions at all frequencies, making the effects of viscosity more important in emulsions than previous results had implied. In figure 18 the recent results obtained by the author have been used. As is seen there, thermal effects are more important at lower frequencies. Viscous effects become dominant in the mid-frequency range, and at high frequencies the acoustic radiation is the largest.

Because of the several differences noted above, it is useful to compare our results to experimental attenuation data. Perhaps the most careful set of experiments that exist for that case are the measurements of Allegra & Hawley in an emulsion composed

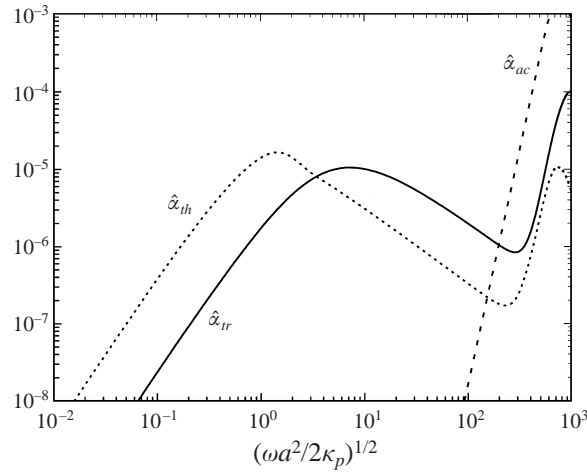


FIGURE 18. Non-dimensional acoustic, thermal and translational attenuations for a very dilute emulsion of $100\ \mu\text{m}$ diameter toluene droplets in water, $\phi_v = 10^{-3}$: ----, acoustic; ·····, thermal; ———, translational.

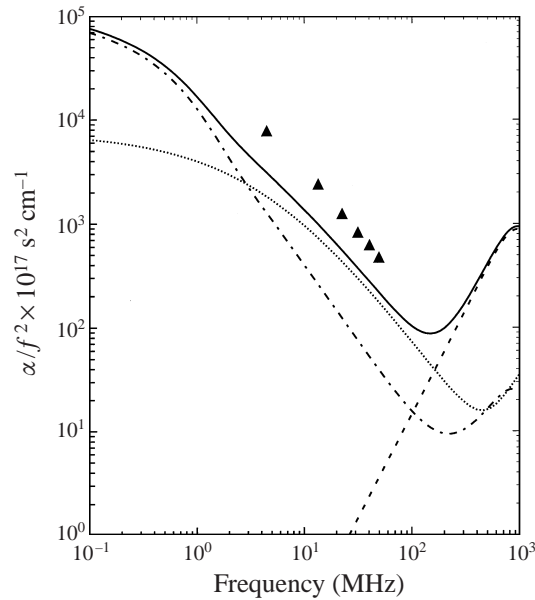


FIGURE 19. Allegra & Hawley's attenuation data in an emulsion of toluene droplets in water having a concentration equal to 0.2 and a diameter of about $7\ \mu\text{m}$. The lines represent dilute attenuation theories: ·····, translational; - · - · - ·, thermal; ----, acoustic; ———, total attenuation.

of $0.3\text{--}0.4\ \mu\text{m}$ radius toluene particles in water. Regrettably, the volume concentration used by them was rather high, 0.2, so that our theory, like that of E & C, is not applicable. Nevertheless, we show in figure 19 a comparison with our results, plotted in the same manner as done by Allegra & Hawley. It is seen that the experimental data follow the same trend as the total attenuation, but have consistently larger values. Given the high concentration in their experiments, the polydisperse nature of the particle size, and the fact that a surfactant was added to stabilize the emulsion, it is surprising to see even a trend agreement.

8. Damping coefficients for gas bubbles

The results obtained in §4 give the temperature and pressure of a fluid particle in a sound wave, and, therefore, specify the response of the particle. However, in the case of gas bubbles, it is customary to describe that response in terms of an effective damping coefficient, which is obtained by writing the response in a manner analogous to that of harmonic oscillator.

Here we obtain the damping coefficient of radially-pulsating particles from the same energy dissipation rates that were used to obtain the attenuation coefficients. The two quantities are of course related, but are defined differently. Thus, the attenuation coefficient represents an energy loss scaled with the energy of the incident wave, whereas the damping coefficient represents the same loss, scaled with the energy that is due to the pulsational motion of the particles.

Thus, when dissipation is small, the attenuation coefficient is defined by (7.1). The damping coefficient, on the other hand, may be defined by

$$\beta = \frac{|\langle \dot{e}_{\text{loss}} \rangle|}{2e_0}, \quad (8.1)$$

where e_0 is the average pulsational energy when the oscillations are stationary. This definition of the damping coefficient also assumes that the dissipation is small.

Now, the average pulsational energy is the total – kinetic plus potential – average energy that exists in both particle and external fluids as a result of the particle pulsations. But for small gas bubbles in liquids, the particle's kinetic energy and the fluid's potential energy may be neglected. Thus, e_0 may be obtained by adding the near-field, or non-acoustic, kinetic energy of the fluid outside the pulsating bubble to the potential energy of the gas in the bubble. The last quantity requires an assumption regarding the thermal behaviour of the gas in the bubble. However, because the oscillations are monochromatic, equipartition of energy applies so that the average kinetic and potential energies are equal. Hence, the total average energy of oscillation is simply twice the average kinetic energy of the fluid resulting from the pulsation. This is known in terms of the added mass and of the radial velocity of the particle surface. Thus (see, for example, Temkin 1981), $e_0 = M_0 |u_s|^2$, where

$$M_0 = 3\rho_{f0}v_{p0} \frac{1}{1+b^2}. \quad (8.2)$$

The radial velocity of the particle was given in (6.2), in terms of the non-dimensional pressure and temperature fluctuations. For simplicity we express that result as $u_s = (i\omega a/3\Psi)(P'_f/\rho_{p0}c_{sp}^2)$, where

$$\Psi = \left[\gamma_p \Pi - \frac{\beta_p \gamma_f - 1}{\beta_f N_s} T \right]^{-1}. \quad (8.3)$$

Thus, substitution of these equations in $e_0 = M_0 |u_s|^2$ yields

$$e_0 = \frac{2}{3\gamma_p} \pi a^3 \frac{(\omega/\omega_{T0})^2}{1+b^2} \frac{N_s}{|\Psi|^2} \frac{|P'_f|^2}{\rho_{f0}c_{sf}^2}, \quad (8.4)$$

where we used $\omega_{s0}^2 = \gamma_p \omega_{T0}^2$ and the definition of ω_{T0}^2 to write $3\rho_{p0}c_{sp}^2$ as $\gamma_p \rho_{f0} \omega_{T0}^2 a^2$. It is important to note that this reference energy, like the dissipation rates, depends on the frequency. Below we use (8.4) to compute the acoustic and thermal damping coefficients. These will be given in the convenient non-dimensional form prescribed

by

$$\hat{d} = \frac{2\beta\omega}{\omega_{T0}^2}. \quad (8.5)$$

Thus, using the definition of β , the acoustic dissipation rate, (6.4), and the reference energy e_0 , we obtain

$$\hat{d}_{ac} = 3\gamma_p(1 + b^2)|\Psi|^2|\Pi - 1|^2/bN_s. \quad (8.6)$$

At low frequencies, this coefficient is essentially equal to the value found in the literature, namely $\hat{d}_{ac} = b(\omega/\omega_{T0})^2$. This value follows by using (3.52) in (8.6).

The thermal dissipation rate is also found using the same procedure. Thus,

$$\hat{d}_{th} = \gamma_p(1 + b^2)|\Psi|^2(\gamma_f - 1)|(\beta_p/\beta_f)\text{Re}(iT\Pi^*) + \text{Re}(iI_f) - \text{Re}(\dot{Q})/2z^2|/N_s, \quad (8.7)$$

which includes both particle and fluid contributions. But as pointed out earlier, for gas bubbles in liquids, the thermal dissipation in the bubble is significantly larger than that in the fluid at all frequencies for which the thermal damping is the dominant mechanism. In that range, we may use for \hat{e}_{th} the simpler result, (6.12), which is entirely due to the particle,

$$\hat{d}_{th} \approx \gamma_p(\gamma_f - 1)(\beta_p/\beta_f)(1 + b^2)|\Psi|^2|\text{Re}(iT\Pi^*)|/3N_s. \quad (8.8)$$

We may express this in a more succinct manner in terms of the quantity κ introduced in §4. Using (4.9), we first write

$$|\Psi|^2|\text{Im}(iT\Pi^*)| = \frac{\xi}{\gamma_p(\gamma_p - 1)} \text{Im}(\kappa), \quad (8.9)$$

where we have used the fact that $\text{Im}(\kappa) \geq 0$. Next, we note that $b^2 \ll 1$, so that on using the definition of ξ , we obtain,

$$\hat{d}_{th} = \text{Im}(\kappa). \quad (8.10)$$

Thus, when we neglect the contributions of the external thermal dissipation, we find that the thermal damping coefficient is simply given by the imaginary part of κ . This is shown graphically in figure 20 for both the uniform-pressure and the general theories. Also shown in the figure are Prosperetti's non-dimensional thermal damping coefficient as well as that predicted by (8.7). This includes the effects of thermal dissipation in the liquid. As discussed earlier, this is important only at high frequencies. In all cases, the theories have been reduced for a 100 μm diameter air bubble in water at STP, as a function of z_p . As anticipated, we see that the uniform-pressure theory agrees with Prosperetti's, except at the lowest frequencies due to temperature fluctuations in the fluid, and that both significantly overestimate thermal damping, for the reasons discussed in §4.

Finally, in figure 21, we show the acoustic and thermal damping coefficients, as well as their sum, which defines the total damping coefficient, as a function of the non-dimensional frequency z_p . This figure shows that acoustic radiation, and not thermal damping, is the dominant mechanism at resonance, a result that was to be expected from our discussion of the energy dissipation rates in §6.

9. Conclusions

This paper has studied the pulsational motions of a small fluid particle immersed in another fluid which is sustaining an acoustic wave. Taking into account the

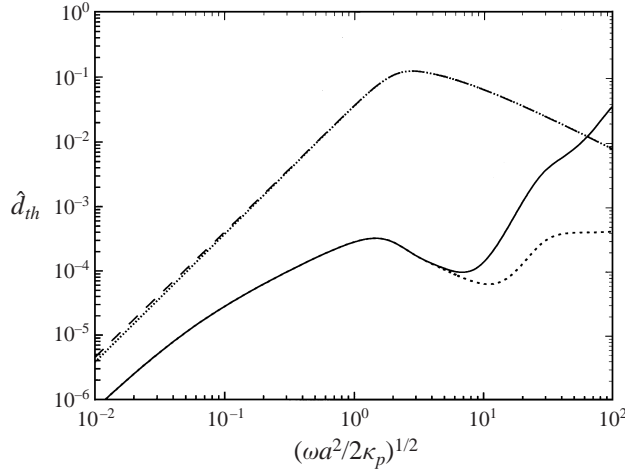


FIGURE 20. Thermal damping for a 100 μm diameter air bubble in water: ----, \hat{d}_{th} , Prosperetti; ·····, $\text{Im}(\kappa)$, uniform pressure theory; - · - · - ·, $\text{Im}(\kappa)$, present results without liquid contribution (equation (8.1)); —, \hat{d}_{th} , general results with liquid contribution.

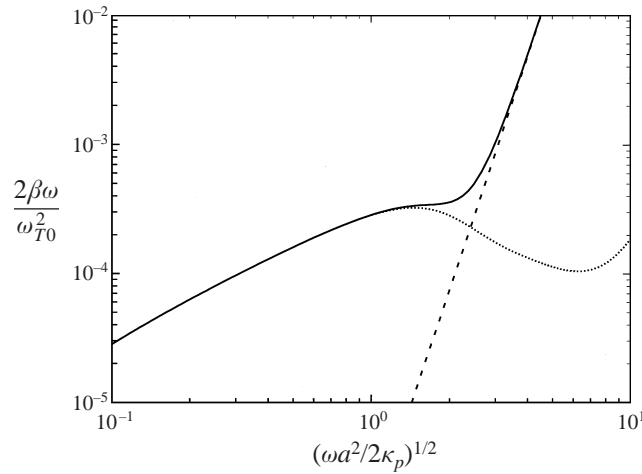


FIGURE 21. Damping coefficients for a 100 μm diameter air bubble in water: ·····, thermal damping; - · - · - ·, acoustic damping; —, total damping.

temperature fluctuations in the external fluid, as well as the pressure and temperature disturbances produced by the pulsating particle, we have derived analytical results for the pressure and temperature oscillation in the particle that are more general than previously available and apply to bubbles in liquids, and to droplets in both liquids and gases. The results are given in terms of the physical properties of both fluids, and of the radius of the particle, and may therefore be used to examine the response in more detail than given here. We also obtained the acoustic and thermal energy dissipation rates, and showed that for gas bubbles the dominant loss mechanism at resonance is acoustic radiation. These rates were used to compute attenuation coefficients in dilute suspensions, as well as damping coefficients for a gas bubble in a liquid. In the case of the acoustic damping, our analysis agrees with existing theories. In the case of the thermal damping our results differ, considerably, from those in

the literature. The differences are due to both the temperature and the pressure fluctuations in the liquid which were not included in previous analysis. Finally, our attenuation results agree with existing theories in the case of droplets in gases, provide a new theoretical framework for attenuation in emulsions, and give the attenuation in very dilute bubbly liquids, where the dissipation rates are small.

I am grateful to referee C whose comments helped clarify several important issues, and to Professor A. Solan of the Israel Institute of Technology for many helpful discussions.

Appendix A. The functions X , Y , U and V appearing in (4.1)

We first introduce the short-hand notation

$$J = b_i^2 G(b_i), \quad \Gamma_R = \text{Re}\{G(q_i)\}, \quad \Gamma_I = \text{Im}\{G(q_i)\}.$$

Then,

$$X = -6Jb(b+z)z^2 + 6(2+z)(J + 3\gamma_p N_s b^2)z^2 - 3J[(\gamma_f - 1)b^2(z-b) + 2z^2] \\ - 3b \left[bJ + 2\frac{\beta_p}{\beta_f} z^2 \right] [bz(\gamma_f - 1) - 2z^2],$$

$$Y = -6(J + \gamma_p N_s b^2)(b+z)z^2 - 6Jb(2+z)z^2 - 3Jb[bz(\gamma_f - 1) - 2z^2] \\ + 3[(\gamma_f - 1)b^2(z-b) + 2z^2] \left[bJ + 2\frac{\beta_p}{\beta_f} z^2 \right],$$

$$U = 2b^2(\gamma_f - 1)Jz^2 \left\{ -\frac{\beta_p}{\beta_f} + \left(\frac{\kappa_f}{\kappa_p} \right) [\Gamma_I(b-z) - \Gamma_R z] \right\} \\ + 2b^2(\gamma_f - 1)z^2 \left(\frac{\kappa_f}{\kappa_p} \right) [\Gamma_R(z-b) - \Gamma_I z] \\ \times \left[bJ + 2\frac{\beta_p}{\beta_f} z^2 \right] - 4(J + \gamma_p b^2 N_s)z^2 z_p^2 [z\Gamma_R - (1+z)\Gamma_I] \\ - 2Jbz^2 \{ 3hz^2 + 2z_p^2 [\Gamma_R(1+z) + z\Gamma_I] \},$$

$$V = 2b^2(\gamma_f - 1)Jz^2 \left(\frac{\kappa_f}{\kappa_p} \right) [\Gamma_R(z-b) - \Gamma_I z] \\ - 2b^2(\gamma_f - 1)z^2 \left\{ -\frac{\beta_p}{\beta_f} + \left(\frac{\kappa_f}{\kappa_p} \right) [\Gamma_I(b-z) - \Gamma_R z] \right\} \\ \times \left[bJ + 2\frac{\beta_p}{\beta_f} z^2 \right] + 4bJz^2 z_p^2 [z\Gamma_R - (1+z)\Gamma_I] \\ - 2(J + \gamma_p b^2 N_s)z^2 \{ 3hz^2 + 2z_p^2 [\Gamma_R(1+z) + z\Gamma_I] \}.$$

Appendix B. The uniform-pressure solution

When pressure variations with position are neglected in both fluids, the corresponding energy equations give, for monochromatic time dependence, the following equations for the non-dimensional temperature disturbances, $\tau_u = (T'_p)_u / \Theta'_f$ for the

particle, and $\tau_f = \theta'_f / \Theta'_f$, for the exterior fluid:

$$\nabla^2 \tau_u + K_i^2 (\tau_u - \xi \Pi_u) = 0, \quad (\text{B } 1)$$

$$\nabla^2 \tau_f + K^2 \tau_f = 0. \quad (\text{B } 2)$$

The boundary conditions are that the temperature and heat fluxes be continuous at the equilibrium surface of the pulsating particle. If τ_s represents the non-dimensional surface fluctuation, the solution of (B 1) satisfying the first condition can be written as

$$\tau_u - \xi \Pi_u = (\tau_s - \xi \Pi_u) \frac{j_0(K_i r)}{j_0(q_i)}. \quad (\text{B } 3)$$

A solution can also be obtained in terms of the second condition. Thus,

$$\tau_u - \xi \Pi_u = \frac{k_f}{k_p} \left(\frac{\partial \tau_f}{\partial y} \right)_{y=1} \frac{j_0(K_i r)}{j_0(q_i)}, \quad (\text{B } 4)$$

where $y = r/a$ and $G(q_i)$ is given by (3.30). Hence

$$\tau_s - \xi \Pi_u = \frac{k_f}{k_p} \left(\frac{\partial \tau_f}{\partial y} \right)_{y=1} G(q_i). \quad (\text{B } 5)$$

We substitute (B 5) into (B 3) and average the result over the equilibrium volume of the particle. This gives

$$\bar{\tau}_u = \xi \Pi_u \left[1 + \frac{3i}{2z_p^2} \frac{k_f/k_p}{\xi \Pi_u} \left(\frac{\partial \tau_f}{\partial y} \right)_{y=1} \right]. \quad (\text{B } 6)$$

To obtain the derivative of the temperature disturbance at the surface of the particle, we use (B 2), the solution of which satisfying the boundary conditions at the surface of the particle and at infinity is

$$\tau_f = (\tau_s - 1) \frac{h_0(Kr)}{h_0(q)}. \quad (\text{B } 7)$$

Taking the derivative of this and evaluating at $r = a$, we obtain, on using (3.24) for $h'_0(q)$,

$$\left(\frac{\partial \tau_f}{\partial y} \right)_{y=1} = (1 - \tau_s)(1 - iq). \quad (\text{B } 8)$$

We now substitute τ_s from (B 5) in this and obtain

$$\left(\frac{\partial \tau_f}{\partial y} \right)_{y=1} = \frac{1 - \xi \Pi_u}{F}, \quad (\text{B } 9)$$

where F is given by (3.40). Substitution of (B 9) into (B 6) yields (4.4).

Appendix C. The integrals I_p and I_f

I_p is defined in terms of $T'_p(r)$ and $p'_p(r)$, which are given by (3.10) and (3.11). For the present purpose it is sufficient to consider

$$p'_p = i\rho_{p0}\omega C j_0(k_i r), \quad T'_p = D j_0(K_i r) / \beta_p \kappa_p. \quad (\text{C } 1a,b)$$

Then we can write I_p as

$$I_p = -i \frac{DC^*}{\Theta'_f(P'_f)^*} \frac{\rho_{p0}\omega}{\beta_p \kappa_p} \frac{1}{b_i q_i^2} \int_0^{q_i} \sin(u) \sin(\lambda u) du, \quad (C2)$$

where λ is complex and is given by $\lambda = b_i/K_i$. This has a small magnitude, so that to order λ^2 we have, upon expansion of I_p , after integration,

$$I_p = -\frac{DC^*}{\Theta'_f(P'_f)^*} \frac{\rho_{p0}\omega}{\beta_p \kappa_p} \frac{\sinh[(1-i)z_p]}{q_i^3 G(q_i)}. \quad (C3)$$

Substituting C and D from (3.16 *a, b*) gives, after some algebra,

$$I_p = \frac{1}{9j_0(b_i)} \left[-b_i^2 G(b_i) T \Pi^* - i \frac{\gamma_f - 1}{\rho_{f0}/\rho_{p0}} \frac{\beta_p \kappa_p}{\beta_f \kappa_f} \frac{\omega \kappa_f}{c_{sf}^2} q_i^2 G(q_i) |T| \right]. \quad (C4)$$

The last term may be neglected, giving (6.11).

For I_f we proceed in the same manner as above. Thus, using the leading terms in the disturbance pressure and temperature in the fluid, namely

$$\pi'_f = i\rho_{f0}\omega A h_0(kr), \quad \theta'_f = B h_0(Kr)/\beta_f \kappa_f, \quad (C5a,b)$$

we can write I_f as

$$I_f = -i \frac{BA^*}{\Theta'_f(P'_f)^*} \frac{\rho_{f0}\omega}{\beta_f \kappa_f} \frac{1}{a^3} \int_a^\infty h_0(Kr) h_0^*(kr) r^2 dr. \quad (C6)$$

Using the explicit value of h_0 to carry out the integration, we obtain

$$I_f = \frac{BA^*}{\Theta'_f(P'_f)^*} \frac{\rho_{f0}\omega}{\beta_f \kappa_f} \frac{h_0(q) h_0^*(b)}{q-b}. \quad (C7)$$

The coefficients B and A are given by (3.15 *a, b*). For A it is sufficient to use only the first term in (3.15 *a*). Substituting these coefficients into (C7) gives

$$I_f = \frac{T'_s - \Theta'_f P'_s - P'_f}{\Theta'_f} \frac{1}{(P'_f)^*} \frac{1}{q-b}. \quad (C8)$$

The final result, (6.18) follows from this by using (3.29) and (3.34).

Appendix D. List of symbols

a	Particle radius
$b = ka$	Non-dimensional pressure wavenumber for external fluid
b_i	Non-dimensional pressure wavenumber for internal fluid
c_{Tf}, c_{Tp}	Isothermal sound speeds in fluid and particle materials
c_{sf}, c_{sp}	Isentropic sound speeds in fluid and particle materials
c_{pf}, c_{pp}	Specific heats at constant pressure
\hat{d}_{th}	Non-dimensional thermal damping coefficient
h	Heat capacity ratio, $2\rho_p c_{pp}/3\rho_f c_{pf}$
K	Thermal wavenumber
$k = \omega/c_s$	Pressure wavenumber based on the external fluid's isentropic sound speed
k_f, k_p	Thermal conductivities
N_s	Ratio of internal to external isentropic compressibilities
N_T	Ratio of internal to external isothermal compressibilities
P'_f	Dilute-suspension fluid pressure fluctuation in a sound wave
p_s	Surface pressure
p'_s	Surface pressure fluctuation
p_f, p_p	Total pressures
$\dot{Q} = \dot{Q}_p/4\pi a k_f \Theta'_f$	Non-dimensional heat transfer rate to a particle
\dot{Q}_p	Heat transfer rate to a particle
$q = (1+i)z$	Value of Ka for interior fluid
$q_i = (1+i)z_p$	Value of Ka for exterior fluid
T_0	Ambient temperature
T_f, T_p	Fluid and particle temperatures
$z = (\omega a^2/2\kappa_f)^{1/2}$	Ratio of particle radius to thermal penetration depth in external fluid
$z_p = (\omega a^2/2\kappa_p)^{1/2}$	Ratio of particle radius to thermal penetration depth in internal fluid
$\hat{\alpha} = \alpha c_s/\omega$	Non-dimensional attenuation
$\hat{\alpha}_{oc}, \hat{\alpha}_{th}$	Non-dimensional acoustic and thermal attenuation coefficient
β_{ac}, β_{th}	Acoustic and thermal damping coefficients
β_f, β_p	Coefficients of thermal expansion
γ_f, γ_p	Specific heat ratios
$\delta_{\kappa_f} = (2\kappa_f/\omega)^{1/2}$	Thermal penetration depth for external fluid
$\delta_{\kappa_p} = (2\kappa_p/\omega)^{1/2}$	Thermal penetration depth for internal fluid
Θ'_f	Dilute-suspension fluid temperature fluctuation in sound wave.
θ'_f	Temperature fluctuation of disturbance produced by particle.
κ_f, κ_p	Thermal diffusivities
μ	Dynamic viscosity
ν_f	Kinematic viscosity
$\xi = \frac{\beta_p/\rho_p c_{pp}}{\beta_f/\rho_f c_{pf}}$	Property ratio
π'_f	Pressure disturbance
ρ_f, ρ_p	Material densities
$\phi = \phi_1 + \phi_2$	Velocity potential
ϕ_1, ϕ_2	Potentials
ϕ_v	Concentration of particles by volume

REFERENCES

- ALLEGRA, J. R. & HAWLEY, S. A. 1972 Attenuation of sound in suspensions and emulsions: theory and experiments. *J. Acoust. Soc. Am.* **51**, 1545–1564.
- BATCHELOR, G. K. 1967 *An Introduction to Fluid Dynamics*. Cambridge University Press.
- COLE III, J. & DOBBINS, R. A. 1970 Propagation of sound through atmospheric fog. *J. Atmos. Sci.* **27**, 426–434.
- EPSTEIN, P. S. 1941 On the absorption of sound by suspensions and emulsions. In *Contributions to Applied Mechanics, Theodore von Kármán Anniversary Volume*, pp. 162–188. California Institute of Technology, Pasadena.
- EPSTEIN, P. S. & CARHART, R. R. 1953 The absorption of sound in suspensions and emulsions. I. Water fog in air. *J. Acoust. Soc. Am.* **25**, 553–565 (referred to herein as E & C).
- FUKUMOTO, Y. & IZUYAMA, T. 1992 Thermal attenuation and dispersion of sound in a periodic emulsion. *Phys. Rev. A* **46**, 4905–4921.
- GUMEROV, N. A., IVANADEV, A. I. & NIGMATULIN, N. A. 1988 Sound waves in monodisperse gas-particle or vapour droplet mixtures. *J. Fluid Mech.* **193**, 53–74.
- ISAKOVICH, M. A. 1948 On the propagation of sound in emulsions. *Zh. Exp. Teor. Fiz.* **18**, 907–912.
- LANDAU, L. D. & LIFSHITZ, E. M. 1959 *Fluid Mechanics*. Pergamon.
- MARBLE, F. 1970 Dusty gases. *Ann. Rev. Fluid Mech.* **2**, 397–446.
- MCCLEMENTS, D. J. & POVEY, M. J. W. 1989 Scattering of ultrasound by emulsions. *J. Phys. D: Appl. Phys.* **22**, 38–47.
- MEDWIN, H. 1977 Acoustical determinations of bubble-size spectra. *J. Acoust. Soc. Am.* **62**, 1041–1044.
- NIGMATULIN, R. I., KHABEEV, N. S. & ZUONG NGOK HAI 1988 Waves in liquids with vapour bubbles. *J. Fluid Mech.* **186**, 85–17.
- PROSPERETTI, A. 1977 Thermal effects and damping mechanisms in the forced radial oscillations of gas bubbles in liquids. *J. Acoust. Soc. Am.* **61**, 17–27.
- PROSPERETTI, A. 1986 Physics of acoustic cavitation. In *Frontiers in Physical Acoustics* (ed. D. Sette), pp. 145–188. North Holland.
- PROSPERETTI, A. 1991 The thermal behaviour of oscillating gas bubbles. *J. Fluid Mech.* **222**, 587–616.
- TEMKIN, S. 1981 *Elements of Acoustics*. J. Wiley & Sons.
- TEMKIN, S. 1990 Dispersion of sound in bubbly liquids via the Kramers–Kronig relationships. *J. Fluid Mech.* **211**, 61–72.
- TEMKIN, S. 1992 Sound speeds in suspensions in thermodynamic equilibrium. *Phys. Fluids A* **4**, 2399–2409.
- TEMKIN, S. 1993 Particle force and heat transfer in a dusty gas sustaining an acoustic wave. *Phys. Fluids A* **5**, 1296–1304.
- TEMKIN, S. 1996 Viscous attenuation of sound in dilute suspensions of rigid particles. *J. Acoust. Soc. Am.* **100**, 825–831.
- TEMKIN, S. 1998 Sound propagation in dilute suspensions of rigid particles. *J. Acoust. Soc. Am.* **103**, 838–849.
- TEMKIN, S. & DOBBINS, R. A. 1966a Attenuation and dispersion of sound by particulate relaxation process. *J. Acoust. Soc. Am.* **40**, 317–324.
- TEMKIN, S. & DOBBINS, R. A. 1966b Measurement of the attenuation and dispersion of sound in an aerosol. *J. Acoust. Soc. Am.* **40**, 1016–1024.
- ÜBERALL, H., GEORGE, J., FARHAN, A. R., MEZZORANI, G., NAGLE, A. & SAGE, K. A. 1979 Dynamics of acoustic resonance scattering from spherical targets: Application to gas bubbles in fluids. *J. Acoust. Soc. Am.* **66**, 1161–1172.
- URICK, R. J. 1948 The absorption of sound of irregular particles. *J. Acoust. Soc. Am.* **20**, 283–289.
- ZINK, J. W. & DELSASSO, L. P. 1958 Attenuation and dispersion of sound by solid particles suspended in a gas. *J. Acoust. Soc. Am.* **30**, 765–771.